UNIVERSITAT DE BARCELONA

ESTUDI GENÈTIC INTEGRAL DE LA REGIÓ 4p15 I IDENTIFICACIÓ DE *PI4K2B* I *STIM2* COM A GENS ALTERATS EN CÀNCER COLORECTAL

Memòria presentada per

Álvaro Aytés Meneses

Per optar al grau de

Doctor per la Universitat de Barcelona

Tesi realitzada sota la direcció del
Dr. Alberto Villanueva Garatachea
Al Laboratori de Recerca Translacional de
L'Institut Català d'Oncologia.

Tesi adscrita al departament de Biologia cel·lular i anatomia patològica
Facultat de Medicina
Universitat de Barcelona
Programa de Biologia i patologia cel·lular (bieni 2001-2003)
Tutor: Dr. Carles Enrich

Alberto Villanueva Carles Enrich Ávaro Aytés

Barcelona, Juny de 2007

Annex

Article sotmés a publicació a *Cancer Cell* (en revisió)

Editorial Manager(tm) for Cancer Cell
Manuscript Draft

Manuscript Number: CC-D-08-00374

Title: **Integrative genomic analysis identifies PI4K2B and STIM2 as commonly altered genes mediating colorectal cancer progression and patient outcome**

Article Type: Research Article

Section/Category:

Keywords: PI4K2B and STIM2; colorectal cancer; 4p14-16; allelic imbalances; beta-catenin/TCF regulation; overexpression; protective tumor cell growth; progression; patient outcome

Corresponding Author: Alberto Villanueva, Ph.D

Corresponding Author's Institution: Institut Català d'Oncologia (ICO)

First Author: Álvaro Aytés, BS

Order of Authors: Álvaro Aytés, BS; David G Molleví, Ph.D; Marga Nadal, Ph.D; Elisabeth Guinó, BS; María Martínez-Iniesta, BS; Laura Padullés, BS; Nuria Baixeras, MD; August Vidal, MD; Sara Puertas, Tecnician; Xavier Solé, BS; Javier García del Muro, MD, Ph.D; Ramón Salazar, MD, Ph.D; Lorna S Johnstone, Ph.D; Enric Condom, MD, Ph.D; Miguel A Peinado, Ph.D; Lluis Espinosa, Ph.D; Victor Moreno, MD, Ph.D; Josep R Germà, MD, Ph.D; Albert Morales, Ph.D; Miguel A Pujana, Ph.D; Gabriel Capella, Md. Ph.D; Alberto Villanueva, Ph.D

INTEGRATIVE GENOMIC ANALYSIS IDENTIFIES *PI4K2B* AND *STIM2* AS COMMONLY ALTERED GENES MEDIATING COLORECTAL CANCER PROGRESSION AND PATIENT OUTCOME

Running Title: *PI4K2B* and *STIM2* involved in colorectal tumorigenesis

Álvaro Aytés [1], David G. Molleví [1], Marga Nadal [1], Elisabeth Guinó [4], María Martínez-Iniesta [1], Laura Padullés [1], Núria Baixeras [1,2], August Vidal [2], Sara Puertas [1], Xavier Solé [4], Javier García del Muro [3], Ramón Salazar [3], Lorna S. Johnstone [8], Enric Condom [2], Miguel Angel Peinado [7], Lluís Espinosa [6], Josep Ramón Germà [3], Víctor Moreno [4], Albert Morales [5], Miguel Angel Pujana [1,4], Gabriel Capella [1] and Alberto Villanueva [1,#].

[1] Translational Research Laboratory, Institut Català d'Oncologia – Institut d'Investigació Biomèdica de Bellvitge (IDIBELL), 08907 L'Hospitalet de Llobregat, Barcelona, Spain.

[2] Pathology Department, Hospital Universitari de Bellvitge - IDIBELL, 08907 L'Hospitalet de Llobregat, Barcelona, Spain.

[3] Medical Oncology Department. Institut Català d'Oncologia - IDIBELL, 08907 L'Hospitalet de Llobregat, Barcelona, Spain.

[4] Bioinformatics and Biostatistics Unit. Institut Català d'Oncologia - IDIBELL, 08907 L'Hospitalet deLlobregat, Barcelona, Spain.

[5] Liver Unit. Institut de Malalties Digestives, Hospital Clínic i Provincial, Institut d'Investigacions Biomèdiques August Pi i Sunyer (IDIBAPS), 08036 Barcelona, Spain

[6] Molecular Oncology Center - IDIBELL, 08907 L'Hospitalet de Llobregat, Barcelona, Spain.

[7] Institut de Medicina Predictiva i Personalitzada del Càncer (IMPPC), Crta Can Ruti, Camí de les Escoles s/n, 08916 Badalona, Barcelona.

[8] School of Biological Sciences, University of Auckland, Auckland, New Zealand

Correspondence to: avillanueva@iconcologia.net
Phone: 34 93 260 7952
Fax:: 34 93 260 74 66

SUMMARY

The complete diagram of molecular perturbations present in colorectal tumorigenesis is far from fully understood. Allelic imbalance is commonly observed at chromosome 4p in colorectal carcinomas and hepatic metastases, but the target gene(s) has yet to be identified. Here, we combined genome mapping in xenografted tumors and transcriptional regulatory predictions to identify critical genes at 4p14-16. We found a cluster of β-catenin/TCF regulation from which *PI4K2B* and *STIM2* were verified by chromatin immunoprecipitation assays. Overexpression of *PI4K2B* and *STIM2* is a common event in colorectal tumorigenesis, and elevated protein or mRNA *PI4K2B* is associated with better patient outcome. *In vitro* siRNA mediated-depletion of either *PI4K2B or STIM2* increases cell proliferation. Therefore, overexpression of these genes is associated with a protective tumor cell growth phenotype, which influences progression, outcome and treatment response.

INTRODUCTION

Colorectal carcinoma (CRC) is the second leading cause of cancer-related mortality in the Western world (Parkin et al., 1993). Prognosis is based on the extent of local invasion through the colon wall, the

presence of lymph node metastases, and distal haematogenous dissemination, mainly to the liver (Deans et al., 1992). The genetic alterations that contribute to CRC development—mainly the activation of oncogenes and inactivation of tumor suppressor genes (Fearon and Vogelstein, 1990; Sjoblom et al., 2006)—are relatively well characterized. However, recurrent somatic genetic alterations may reveal additional genes that participate in the neoplastic process but have not yet been identified. Allelic imbalances detected as recurrent loss of heterozygosity (LOH) at polymorphic loci are among the most frequent alterations of this type.

Previous studies have reported allelic losses on one or both arms of chromosome 4 in several tumor types (Pershouse et al., 1997a; Piao et al., 1998; Sherwood et al., 2000; Shivapurkar et al., 1999). Karyotyping or comparative genomic hybridization (CGH) (Grade et al., 2006) analysis of colorectal tumors identified distinct gained or lost regions. Similarly, DNA fingerprints generated by arbitrarily-primed polymerase chain reaction of paired normal and tumor tissues revealed recurrent allelic imbalances at chromosome 4 (4p14-16 and 4q21-28) (Arribas et al., 1999b). In addition, Shivapurkar et al. (Shivapurkar et al., 2001) identified two regions of frequent LOH at 4p15 and 4p16.

A recent meta-analysis of CGH data showed that LOH at 4p was associated with the transition from Dukes' stage A to stages B-D (Diep et al., 2006). This is in line with the increased LOH frequency at 4p reported in metastases when compared with primary colorectal carcinomas (Malkhosyan et al., 1998). In fact, allelic imbalances in this region have been associated with poor prognostic (Arribas et al., 1999b; Bardi et al., 2004). The presence of LOH at 4p has been also associated with a more aggressive phenotype in other tumor types (Polascik et al., 1995; Sherwood et al., 2000).

To identify cancer genes at 4p14-p16, we generated a library of xenografted primary colorectal tumors and hepatic metastases in nude mice. Fine genomic mapping of these xenografts and primary tumors identified a critical region of six megabases (Mb) of LOH, named region A, which contained ten candidate tumor suppressor genes. To determine which of these genes would be more likely to mediate colorectal tumorigenesis, we examined transcript profiles and predicted transcriptional regulatory associations in relation to members of the Wnt signaling pathway. These predictions identified *PI4K2B* and *STIM2* as putative ß-catenin/TCF target genes. Extensive analysis of these two genes revealed roles in progression, patient outcome and chemotherapy response. This study improves knowledge of common genetic alterations and molecular mechanisms of colorectal cancer. The strategy applied here could also be useful in identifying other cancer genes in recurrently altered regions of tumor genomes.

RESULTS

Generation of colorectal tumors and hepatic metastases xenografted in nude mice

Forty-six of 73 (63%) colorectal tumors (CRC) [(41/46 (89.1%) colon; five of 46 (10.8%) rectum)] and 20 of 22 (91%) hepatic metastases (HM) (6 synchronous and 14 metachronous) developed as tumor xenografts in nude mice (**Table S1** and **Table S2** available online). Implanted CRC were mainly Dukes' stages B and C (**Table S3** available online). To obtain *in vivo* distal dissemination, twenty-three CRC were also orthotopically implanted in the *ceacum* of the mice, and macroscopic distal metastases were obtained in nine tumors (three peritoneal implants, two lung metastases and four hepatic metastases were generated) (**Table S1**). Histological analysis of xenografted tumors (CRC-X and HM-X) confirmed primary diagnosis of adenocarcinoma and the colorectal origin of hepatic metastases. This collection of xenografts is a useful tool for detailed genetic profiling.

Complex allelic imbalances are present at 4p14-16 in CRC and HM

To investigate the allelic status of the 4p14-16 region, we performed an extensive study of LOH of microsatellite markers spanning a 15.2-Mb region (**Figure S1A** available online) in matched cases of (i) normal colorectal mucosa/CRC/CRC xenograft (CRC-X) and (ii) liver parenchyma/HM/HM xenograft (HM-X). This approach shows

greater sensitivity and specificity because the xenografts are not affected by human stromal contamination (Caldas et al., 1994) . Using an initial limited set of representative 4p14-16 markers, allelic imbalances were observed in 13 of 46 (28.3%) xenografted CRCs (**Figure S1B** and **S1C**). An extensive LOH study revealed a complex genetic pattern with discrete subregions (**Figure 1A**), and retention of the heterozygotic state in the inter-regions was confirmed by fluorescent labeled primers and analysis with GeneMapper 3.0 (**Figure S1D**). Despite this pattern, a clear imbalance at marker D4S2397 was observed in all 13 xenografts with LOH. Thus, we performed an in-depth genomic analysis by focusing on a 6-Mb region centered by this microsatellite marker (region A).

Twenty-five percent (five of 20) of xenografted HMs showed LOH at 4p14-16. Unlike the primary CRC, a simpler pattern of LOH was observed in HM, and a range of one to three subregions with no additional telomeric LOH was identified (**Figure 1B**). We next examined whether LOH at 4p14-16 was selected during distal dissemination in nude mice. No additional allelic imbalance was detected in the 17 metastases obtained from tumor xenografts with or without LOH (**Figure 1C**). These data suggest that allelic imbalances at 4p14-16 are early events in colorectal tumorigenesis.

A total of 15 tumor xenografts with LOH (ten CRC-X and five HM-X) and 15 without LOH (ten CRC-X and five HM-X) at 4p14-16 were selected for a more detailed genetic analysis of region A.

Candidate genes in region A lack inactivating somatic mutations

Information from human genome databases revealed the presence of 14 genes in region A. Ten of these 14 genes share high homology with orthologous mouse genes located in a synthetic region on chromosome 5. The genes, ordered from telomere to centromere, were: *PI4K2B* (*phosphatidylinositol 4-kinase type-II beta*), *ZCCHC4* (*zing finger, CCHC domain containing 4*), *ANAPC4* (*anaphase promoting complex subunit 4*), *SLC34A2* (*solute carrier family 34 (sodium phosphate) member 2*), *KIAA0746* (*KIAA0746 protein*), *LOC389203* (*hypothetical gene supported by BC032431*), *RBPSUH* (*recombining binding protein suppressor of hairless*), *CCKAR* (*cholecystokinin A receptor*), *FLJ11082* (*hypothetical protein FLJ11082*) and *STIM2* (*stromal interaction molecule 2*).

To determine whether any of the candidate genes identified in this region may harbor somatic mutations, we performed an extensive mutational genetic analysis of the ten selected genes in the set of 15 xenografts harboring LOH. Neither somatic point mutations, microdeletions, nor homozygous deletions were identified by direct sequencing and SSCP analysis in the group of xenografts showing LOH. These results rule out the presence of a second genetic hit, which is characteristic of standard tumor suppressor genes.

An integrative genomic approach identifies *PI4K2B* and *STIM2* as ß-catenin/TCF target genes

To identify critical colorectal cancer genes in region A, we examined correlations between transcript profiles and canonical genes of the Wnt signaling pathway that may reveal functional associations. Using the Pearson correlation coefficient (PCC), high metric correlations (positive or negative) were observed between several genes in region A and the transcription factor (TF) *TCF4* (**Figure 2A**). To further assess the significance of these correlations, we examined PCCs between *TCF4* and 10,000 randomly chosen equivalent gene sets. The average correlation of the genes in region A was in the 76th percentile in the human transcriptome, which suggests that some of the genes in this region may be TCF4 targets.

Next, we examined a regulatory network using 295 microarray hybridizations of human CRCs to determine whether these higher correlations represent direct transcriptional regulations by TCF4 or other Wnt-related TFs. Stringent associations in this network predicted regulations of TCF4 and/or other Wnt-related TFs such as SMAD4, TCF3 and TCF25 with five genes in region A (**Figure 2B**). Of these genes, *PI4K2B* and *STIM2* were predicted to be associated with three or two TFs, respectively. To obtain experimental verification of these predictions, we performed β-catenin chromatin immunoprecipitation (ChIP) assays for TCF binding sites in TRANSFAC at the promoters

of *PI4K2B and STIM2*. Comparison between non-CRC and CRC cell lines suggests that both genes are regulated by β-catenin (**Figure 2C**). Taken together, the analysis of transcript profiles in CRCs, predicted regulatory associations and experimental verifications indicate that *PI4K2B* and *STIM2* may be targets of common genetic alterations in CRC in region A.

Overexpression of *PI4K2B* and *STIM2* mRNA is a common event in human colorectal tumorigenesis

We performed quantitative PCR (qPCR) to determine whether allelic imbalances were associated with aberrant regulation of *PI4K2B* and *STIM2* expression levels in the ten matched cases of normal colon mucosa and colorectal tumor xenografts harboring LOH. An overall increase in mRNA expression was observed for *PI4K2B* (fold change 5.37) and *STIM2* (fold change 2.35) (**Figure 3A and 3B** upper panel); this overexpression was already present in their matched primary tumors. Notably, overexpression was independent of allelic imbalances (**Figure 3A and 3B** lower panel). Overexpression of CRC9A (without LOH) and CRC9B (with LOH) was observed in two independent tumors originated from the same patient (**Figure 3B**).

The degree of overexpression was only significant for *STIM2* and *PI4K2B* (**Figure 3C**), while the increased levels of *ANAPC4* (P = 0.40), *KIAA0746* (P = 0.14) and *RBPSUH* (P = 0.17) did not reach significance. As shown in **Figure 3A** lower panel, similar expression behavior was observed for the tumors without LOH, which reached significance for *PI4K2B* (fold change 8.74) and *STIM2* (fold change 2.84) (**Figure 3C**). Thus, overexpression of *PI4K2B* and *STIM2* with respect to paired normal colon mucosa was consistently detected in the majority of tumors analyzed. This overexpression was also present in the set of HM: *PI4K2B* (fold change 5.37) and *STIM2* (fold change 3.81) (**Figure 3D**). Three additional genes in region A *(ANAPC4*, *KIAA0746* and *RBPSUH*) also showed increased levels of expression in HM, although the differences did not reach statistical significance. Extremely low or undetectable expression levels were found for the remaining genes in region A *(CCKAR*, F*LJ11082*, *LOC389203*, *SLC34A2* and *ZCCHC4)* in normal mucosas and CRC or HM. Together, these results provide experimental confirmation that *PI4K2B* and *STIM2* overexpression are common events in colorectal tumorigenesis.

Expression changes are not regulated by methylation of gene promoter CpG islands

The methylation status of the 5' CpG islands was examined to assess whether overexpression changes for *PI4K2B* and *STIM2* can be regulated by promoter hypomethylation status. No change in methylation pattern was observed between paired normal mucosa and tumors (**Figure S2** available online).

LOH at 4p14-16 does not correlate with loss of genetic material by FISH

The unexpected overexpression results identified in tumors with LOH by microsatellite markers led us to re-examine the tumor ploidy. Primary tumors and paired xenografts of both groups of CRC (with and without LOH) were hybridized with pairs of fluorescent probes (*RP11-372F2* and *RP11-293A21*; *RP11-473F10* and *RP11-475J10*) (**Figure 4A**). **Table S4** online summarizes the results of the FISH analysis. All tumors without LOH were diploid in region A with the exception of CRC7, which had 20% tetraploid nuclei. Seven of ten cases (70%) with LOH were diploid. An example of the discrepancy between microsatellite LOH data and FISH results is shown in **Figure 4B**. Only two (CRC19 and CRC28) of ten tumors (20%) were haploid, showing a deletion of the region containing the two genes (**Figure 4C**), whereas one of the ten (10%) was near-diploid (CRC24, 18% triploid nuclei). Consistent results were observed in paired primary CRCs. For the HMs, a deletion in the region containing *STIM2* was identified in one (HM10) of five cases, two others (HM12 and HM15) were near-triploid, and the remaining cases (HM3 and HM20) were diploid (**Figure 4C**). Thus, our results show that expression changes are independent of tumor cell ploidy in most cases of CRC and HM.

Levels of PI4K2B protein and mRNA have clinical relevance in CRC

To determine to possible prognostic value of PI4K2B and STIM2 expression levels, we performed immunoshistochemistry (IHC) on a tissue microarray (TMA) of colorectal tumor. **Figure 5A** shows examples of

immunostaining for both genes. For PI4K2B, 101 cases yielded informative results. Excellent agreement was observed between TMA and standard whole-section IHC analyses. Decreased intensity of PI4K2B protein expression showed an association with poor overall survival (OS) (Low intensity + or - *vs.* High intensity ++ or +++) (*P* = 0.047; Hazard Ratio (HR) = 1.89; 95% Confidence Interval (CI) = 1.01-3.52) (**Table 1**; **Figure 5B** upper graph). Patients with tumors harboring a lower percentage of cells expressing for PI4K2B was not associated with prognosis (<10% of tumor cells expressing PI4K2B; *P* = 0.53; HR = 1.29; CI = 0.59-2.83). When both variables were combined in an IHC score, a significant OS association was observed (*P* = 0.021; HR = 2.12; CI = 1.13-3.97) (**Figure 5B** middle graph). A similar trend was observed for shorter disease-free survival (DFS) (**Table 1**; **Figure 5B** lower graph).

For STIM2, 113 cases yielded informative results. A diffuse cytoplasmatic immunostaining was observed and good agreement was found between TMA and paired whole-tumor sections. No association was observed when immunostaining intensity or the percentage of positive cells and patient outcome were considered. No additional information was obtained when PI4K2B and STIM2 immunostaining were considered together (**Table 1**).

In a randomly selected group of 25 cases, an excellent correlation was observed for both genes between protein and mRNA expression levels determined by IHQ and qPCR respectively.

To determine whether *PI4K2B* and *STIM2* expression may also have a predictive value in 5-FU-based chemotherapy response, we conducted qPCR to measure the mRNA levels of both genes in a consecutive series of 140 colorectal tumor patients treated adjuvantly with 5-Fluorouracil (5-FU)-based chemotherapy. Normalized expression ratios between matched primary tumors and normal colonic mucosa were calculated for *PI4K2B* and *STIM2* genes, and the median value was established as the cut-off. Low *PI4K2B* expression levels were associated with diminished disease-free survival (DFS) (*P* = 0.027; HR = 2.25; CI = 1.07-4.7) (**Figure 5C** lower graph; **Table 2**). A similar trend was observed for overall survival (*P* = 0.068; HR = 1.72; CI = 0.95-3.1) (**Figure 5C** upper graph). Similarly to the prognostic setting, no association was observed between *STIM2* mRNA expression levels and OS (p = 0.94) or DFS (p = 0.64). Finally, no additive or synergistic effect was found when both genes were considered (**Table 2**).

siRNA-mediated depletion of *PI4K2B* and *STIM2* reveals a cell growth suppressor phenotype

Our results revealed that *PI4K2B* and *STIM2* overexpression are common events in colorectal tumorigenesis irrespective of the presence of allelic imbalances. Paradoxically, those tumours with diminished expression were associated with a worse prognosis. To determine the function of these genes, siRNA silencing assays were performed on a colorectal DLD-1 cell line exhibiting high expression levels for both genes (**Figure 6A**). The assays showed a significant reduction in gene expression for *STIM2* or *PI4K2B* (**Figure 6B and 6D**), which was associated with a significant increase in cell growth (60% increase for *PI4K2B*: *P* < 0.01; *n* = 3; and 45% increase for *STIM2*: *P* < 0.01; *n* = 3) (**Figure 6C and 6E**). These results suggest a cell growth suppressor phenotype for both genes, and are in agreement with the better outcome observed in patients with tumors showing increased levels of these proteins.

DISCUSSION

Chromosome 4 genetic alterations make a clear contribution to the onset and progression of different tumor types. Genetic (Arribas et al., 1999a; Arribas et al., 1999b; Shivapurkar et al., 2001) and functional (Pershouse et al., 1997b) analyses indicate that chromosome 4 is likely to contain several mutated or aberrantly expressed genes that may play a role in tumorigenesis. By combining comprehensive genetic analyses in tumor xenografts derived from primary CRCs and HMs, examination of transcript profiles and their regulation, tumor cell line siRNA assays, and expression studies on well characterized tumor patient series, we identified *PI4K2B* and *STIM2* as CRC target genes. Overexpression of both genes was associated with a protective tumor cell growth phenotype. Furthermore, we showed that aberrant PI4K2B expression may have a clinical impact.

Our refined LOH analysis revealed that the 4p14-16 region harbors a complex pattern of allelic imbalances. The prevalence of LOH observed in our study is lower than previously reported (Shivapurkar et al., 2001), which is probably due to the increased number of markers used in the present study and the clear interpretation of LOH results in xenografts. The similar prevalence of LOH in hepatic metastases and primary tumors suggests that this alteration is an early event that does not confer growth advantage during distal dissemination.

In the colorectal tumors, the allelic imbalances identified by LOH at 4p14-16 were rarely associated with loss of genetic material. Only three of 15 tumors (two CRC and one HM) displaying LOH by microsatellite analysis were truly haploid. Thiagalingam et al. conducted whole painting FISH of colorectal tumor xenografts with LOH and showed that complete loss of chromosomes 5, 8 or 17 as detected by allelotyping was associated with duplication or triplication of the remaining chromosome, while partial chromosome losses were associated with gross structural changes associated with interchromosomal recombination (Thiagalingam et al., 2001). Several basic mechanisms have been considered to account for LOH: chromosomal non-disjunction, mitotic recombination or deletion, and gene conversion or point mutation (Cappione et al., 1997; Cavenee et al., 1985; Stanbridge, 1990). Thus, whereas the high number of LOH subregions in the CRC may be the result of multiple recombination events, the imbalance of the entire 4p14-16 region in hepatic metastasis might be consistent with a non-disjunction process.

An integrative genomics approach using colorectal cancer expression profiles identified *PI4K2B* and *STIM2* as ß-catenin/TCF target genes in the selected region. TCF/LEF is a nuclear binding partner of ß-catenin that mediates transcriptional regulation of Wnt target genes (Reya and Clevers, 2005). In line with our prediction, both *PI4K2B* and *STIM2* were significantly overexpressed in tumor samples. Interestingly, overexpression occurred in most cases of CRC independently of LOH status, and in the absence of somatic genetic alterations. β-catenin ChIP assays confirmed that this regulation occurs in colorectal cancer cell lines. Predicted direct transcriptional regulatory interactions also identified other interactions, which suggest that STIM2 may play a role in the cross-talk between other signaling pathways. Note that we ruled out any type of epigenetic methylation promoter change in the genes analyzed, which might individually or coordinately regulate expression in the area of study, as recently described in colorectal cancer (Frigola et al., 2006).

To our knowledge, this is the first report to associate both genes with colorectal cancer. While no information is available on the link between *PI4K2B* and cancer, *STIM2* is amplified and overexpressed in glioblastoma multiforme (Ruano et al., 2006). STIM2 has been placed at the center of a feedback that maintains basal cytosolic and endoplasmatic reticulum (ER) Ca^{2+} concentrations within tight limits (Brandman et al., 2007; Parvez et al., 2008; Williams et al., 2001). STIM2 and STIM1, the other family member, play a coordinated role in controlling SOC-mediated Ca^{2}+ entry signals (Liou et al., 2005). Whereas STIM1 is a required mediator of SOC activation, STIM2 is a powerful inhibitor of this process (Soboloff et al., 2006). *STIM1* has been identified *in vitro* as a potential tumor suppressor gene in rhabdomyosarcomas (Sabbioni et al., 1997; Sabbioni et al., 1999), and as a candidate metastasis-related gene (Suyama et al., 2004). We hypothesize that changes in the level of *STIM2* expression may have a significant impact on the direct control of Ca^{2+} levels regulated by the coupled STIM1/STIM2 proteins, which disturbs the regulation of a number of different cell processes.

Phosphatidylinositol 4-kinase type 2 beta (PI4K2B) is a member of the PI4-kinase (PI4K) family that catalyzes the phosphorylation of phophatidylinositol at the 4' position to produce phosphatidylinositol 4-monophosphate (PI(4)P), which is then converted to phosphatidylinositol 4,5-bisphohate (PI(4,5)P2) by PIP5-Kinase (PIP5K) (Fruman et al., 1998). PI(4,5)P2 serves as a precursor for two well-defined second messengers (Berridge, 1987): diacyldlycerol (DAG), which activates PKC (Nishizuka, 1984), and inositol 1,4,5-triphosphate (IP3), which mobilizes Ca^{2+} from intracellular stores. We hypothesize that imbalances in the pool of the phosphatidylinositol PI(4)P or PI(4,5)P2

generated by increased activity of *PI4K2B* may directly alter the intracellular concentration levels of IP3, the end product of the PI3K pathway, also altering Ca^{2+}-regulating signaling pathways.

Overexpression of both genes is a common event in CRC and occurs independently of the allelic imbalance status of the 4p14-16 region, with high levels of expression associated with a protective tumor cell growth phenotype. While siRNA experiments point to a tumor growth suppressor role for both genes, the level of expression only has prognostic relevance in CRC in the case of *PI4K2B*. Despite their functional impact, *PI4K2B* and *STIM2* cannot be easily classified as conventional tumor suppressor genes, which is in line with the fact that mapping regions of recurrent LOH has seldom succeeded in validating Knudson's two-hit hypothesis for candidate genes harboring somatic mutations. Both tumor heterogeneity and the extent of aneuploidy, polyploidy, and complex karyotypes in tumor cells may account for this failure (Dutrillaux et al., 1991; Tomlinson et al., 2002). The complex role envisioned for both genes may also account for the lack of genetic and epigenetic alterations, as well as pointing to the existence of other, more flexible genetic regulatory mechanisms. We suggest that *PI4K2B* and *STIM2* belong to a new category of genes that share the ability to block tumor cell growth with tumor suppressor genes. Nevertheless, unlike tumor suppressor genes that exhibit the phenotype when both alleles are functionally turned off, *PI4K2B* and *STIM2* appear to regulate tumor cell growth when they are overexpressed.

Patients with increased mRNA levels of *PI4K2B* showed a better 5-FU-based chemotherapy response, suggesting that phosphatidylinositol levels generated by the PI4K signaling pathway may have a role in the mechanisms of resistance to 5-FU chemotherapy. Treatment of ovarian cancer cell lines with orobol, an inhibitor of PI4K, increases the sensitivity to cisplatin (Shiotsuka and Isonishi, 2001). Further experiments must be performed to clarify the relationship with colorectal chemotherapy.

Our study demonstrates that recurrent regions of LOH are good indicators of the presence of genes relevant to tumorigenesis, independently to the classical conception of tumor suppressor genes as characterized by the presence of two hits of gene function inactivation. The existence of other, more flexible genetic regulatory mechanisms may account for other genes that give relevance to these regions. Accordingly, we believe that similar comprehensive experimental approaches will be useful in identifying new relevant genes in other frequently disrupted chromosome regions.

In summary, we identified *PI4K2B* and *STIM2* as two genes with a tumor cell growth suppressor phenotype in colorectal cancer and found that both are ß-catenin/TCF target genes. *PI4K2B* overexpression was associated with prognosis and response to 5-FU chemotherapy. Both proteins are functionally related to the Ca^{2+}- signaling pathway, which supports the key role of Ca^{2+}- regulated signaling pathways in colorectal tumor development. Further studies should be carried out to clarify this role and the relationship with other members of the Wnt signaling pathway in CRC.

MATERIALS AND METHODS

Human colorectal carcinomas and hepatic metastases

Fresh surgical specimens of a continuous series of 73 human colorectal carcinomas and 22 hepatic metastases were obtained after surgical resection at the Hospital Universitari de Bellvitge, Barcelona (Spain) between January 2000 and December 2001. Paired normal colon mucosa and liver parenchyma were available for all cases. **Table S3** summarizes the clinicopathological features of CRC and HM patients, while individual tumor characteristics are shown in **Table S1** and **Table S2**. None of the colorectal cancer patients had received previous cytotoxic chemotherapy treatment, and for the cases of metachronous hepatic metastases, at least six months were given before hepatectomy when receiving 5-FU adjuvant chemotherapy.

Cell lines and reagents

HEK-293, HS-27, HeLa, HCT-116, SW480, HT-29 and DLD-1 were cultured in DMEM 10%

FBS at 37ºC and 5% CO_2. Transfection of DLD-1 was performed with lipofectamine 2000® at 60-80% confluence.

Generation of xenografted colorectal and hepatic metastasis in nude mice

Tumor samples were placed in DMEM medium supplemented with 10% FCS and penicillin/streptomycin. Animals were housed in a sterile environment, cages and water were autoclaved, and bedding and food were γ-ray sterilized. Five-week-old male *nu/nu Swiss* mice (Harlam, France) weighting 18-22 g were used for each tumor implantation. Nude mice were anesthetized by isoflurane inhalation. For all cases (*n* = 73 CRC; n = 22 MH), two pieces of 2-5 mm^3 were implanted subcutaneously in two different mice. Two small incisions were made in each flank, the tumor introduced, and the incision closed with surgical staples. To obtain distal metastases, 25 of the primary colorectal tumors were simultaneously implanted in the *ceacum* of nude mice after a left lateral laparotomy. Tumor pieces were anchored to the *ceacum* surface with a Prolene 6.0 suture, as described previously (Tarafa et al., 2000). The abdominal incision was closed with 4.0 Vicryl. Mice were inspected twice a week and kept alive until moribund. When no tumor growth was apparent, mice were sacrificed six months after implantation. A good correlation was observed between the histological appearance of the primary tumors and xenografts. All experiments with mice were approved by the Institutional Animal Care and Use Committee.

Genetic and epigenetic analysis

DNA was extracted from human tumors (CRC and HM), colorectal and hepatic xenografts (CRC-X and HM-X), and paired normal colon mucosa or hepatic parenchyma, following standard phenol-chloroform protocols. Nude mouse liver tissue was included in all PCR experiments to rule out contamination by mouse DNA.

Loss of heterozygosity (LOH) analysis: Thirty microsatellite markers were selected from the human uniSTS database, mapping a 15.2-Mb region of 4p14-16. For hepatic metastases, a total region of 30 Mb was examined using an additional set of 27 distal markers. Microsatellite marker location, oligonucleotides, and PCR conditions are provided in **Table S5** available online. All PCR reactions were carried out using 100-200 ng of genomic DNA in a mixture containing PCR reaction buffer, 125 µM of each deoxynucleotide triphosphate, 1 µM primer, 2.5 mM $MgCl_2$ and 1 unit of Taq DNA polymerase (Invitrogen) in a final volume of 30 µl. Annealing temperature, extension time and concentration of $MgCl_2$ were optimized for each primer set, and PCR products were diluted 1:5 in formamide-dye loading buffer, incubated for 4 min at 95ºC, cooled on ice, and loaded onto 6-8% polyacrylamide 8 M urea denaturing sequencing gels. Electrophoresis was carried out at room temperature under 55 W for 2-3 h and gels were silver stained. LOH was defined by total loss of one allele or by a clear decrease in intensity apparent on naked-eye inspection in any of the alleles analyzed. Retention of heterozygosity for flanking markers defining subregions of LOH was confirmed with fluorescent labeled oligonucleotides and capillary electrophoresis in an ABI Prism 3770 sequencer and analyzed with the GeneMapper 3.0 software (**Table S5**).

Detection of point mutations: We analyzed the whole coding sequence of *PI4K2B* (10 exons); *ZCCHC4* (13 exons); *ANAPC4* (22 exons); *SLC34A2* (24 exons); *KIAA0746* (23 exons); *LOC389203* (4 exons); *RBPSUH* (11 exons); *CCKAR* (5 exons); *FLJ11802* (21 exons) and *STIM2* (12 exons). All exons were amplified in independent PCR reactions using human intronic primers (Primers and PCR conditions are available on request). Reactions were carried out using 100-200 ng of genomic DNA in a mixture containing PCR buffer, 100 mM deoxynucleotide triphosphates, 0.5 µM of each primer and 1 unit of Taq DNA polymerase (Invitrogen). The presence of gene mutations was determined by (i) direct sequencing of purified PCR products, and (ii) single strand conformation polymorphism (SSCP) analysis. PCR products were diluted 1:4 in formamide-dye loading buffer and incubated for 3 min at 95ºC, cooled on ice, and loaded onto 6-8% non-denaturing sequencing gel. Electrophoresis was carried out at room temperature under 7-9 W for 12-14 hours. Gels were silver stained. Shifted single-strand bands were excised, re-amplified and sequenced. When mouse DNA co-amplification occurred, the human

product was gel-purified prior to genetic analysis.

The presence of homozygous deletions or microdeletions was evaluated in agarose gels after amplification of the different gene exons. A possible homozygous deletion was defined by the absence of PCR product in three independent experiments, as described previously.

CpG methylation studies: DNA bisulfite reaction was carried out in 2 µg of restriction-digested DNA for 16h at 55ºC under the conditions described previously (Frigola et al., 2006). CpG islands were identified and selected using information available from the UCSC Genome Browser on Human Map 2006 Assembly (http://www.genome.ucsc.edu). **Figure S2** shows the genomic location of the CpG islands analyzed. The primers used for CpG analysis are listed in **Table S6** available online**.** Methylation studies were performed comparing the methylation pattern between normal mucosa and both primary (CRC and HM) and xenografted (CRC-X and HM-X) tumors. Briefly, 100-250 ng of DNA was amplified and the product was diluted 1:50 in distilled water. Nested PCR was performed with 5 µl of diluted product. Three independent PCRs were performed and products were pooled to ensure a representative methylation profile. The PCR products and five individual clones from the TOPO system (Invitrogen) were sequenced.

Fluorescence in situ hybridization (FISH) in tumor imprints: A small piece (approximately 3 mm^3) of tissue was cut and placed on a clean slide. Slight pressure was applied to the tissue to create the imprint and slides were dried at room temperature. Imprints were completely covered with methanol: acetic acid (3:1) mixture and allowed to dry under a light bulb in a smoke hood until complete evaporation of the fixative solution. Once dry, the slides were placed in an oven at 55ºC for 30 min for hybridization. Fluorescence *in situ* hybridization (FISH) was performed as described elsewhere (Nadal et al., 1997). Briefly, four different probes based on chromosome 4p were used to assess the complete or partial loss of the short arm of chromosome 4: RP11-372F2 (4p16.3, close to the telomere located between 2.957.934 and 3.141.096 nucleotides (nt)); RP11-293A21 (4p15.2, containing the *STIM2* gene located between 26,457,152 and 26,637,886 nt); RP11-473F10 (4p, containing the *PI4K2B* gene located between 24,937,712 and 25,071,126 nt; and RP11-475J10 (4p13, close to the centromere located between 45,382,013 and 45,553,406 nt). All probes were obtained from the 32K BAC library (kindly provided by Dr. L. Pérez-Jurado), and the identity of each clone was confirmed by sequencing of the insert ends. Hybridizations were made in pairs: RP11-372F2 with RP11-293A21 and RP11-473F10 with RP11-475J10. One µg of each probe was labeled, co-precipitated with 1 µg or 10 µg of human Cot1 DNA (GIBCO) and diluted in a hybridization mix. Slides were incubated overnight with 10 µl of the hybridization mix in a humid chamber at 37 ºC. Post-hybridization washes were performed by soaking the slides in 0.4 X SSC / 0.1 % Tween 20 at 74 ºC for 2 min and then in 2 X SSC / 0.1 % Tween 20 for 2 min at room temperature. Finally, slides were mounted in 40 µl of Vectashield antifade solution (Vector Laboratories) containing 150 ng/ml of DAPI stain. Mouse colon imprint was added as a negative control. Hybridization spots were counted using a fluorescence microscope (Olympus, BX60) equipped with the appropriate filter set. A total of 100 non-overlapping nuclei showing clear signals were scored for hybridization.

Quantitative real-time PCR (qPCR)

Total RNA was extracted from normal, primary and xenografted tumors using TRIZOL reagent following manufacturers' instructions (Invitrogen). Five hundred ng of total RNA was reverse transcribed to cDNA using $p(dT)_{11-18}$ and the M-MLV retrotranscriptase kit (Invitrogen). Quantitative real-time PCR (qPCR) was carried out using the LightCycler 480 system (Roche). Briefly, 1µl of 1:5 diluted cDNA was added to a 10 µl final volume containing 2.5 mM $MgCl_2$, 1 µM of primers and 1 µl of SYBR Green 1 Master Mix (Roche). Primer for human PCR amplifications were: *STIM2* 5'-TGACAGACCGGAGTCATC-3' and 5'-CGGTGTAACCCCTCCAAG-3'; *PI4K2B* 5'-AGAAATACAGACAGGGGC-3' and 5'-TCCATTTTGATTCCTTATGG-3'; ANAPC4 5'-TTTAAAATTGCTCGAGTC-3' and 5'-TGAAGCACCATTGGTAGAG-3'; RBPSUH 5'-CAGTGGGGAGCCTTTTTT-3' and 5'-TGGATGTAGCCATCTCGG-3'; KIAA0746 5'-

TTAGAAGATTCTTAGTAC-3' and 5'-ACTTGCTGCATATTCCG-3'.

To avoid cross-amplification with the mouse RNA and to prevent DNA amplification, all primers were designed following two premises: (i) located on two different exons; and (ii) with selective amplification of the human cDNA sequence.

All reactions were performed independently in triplicate using three RNA isolates. The human *β_2-microglobulin* housekeeping gene was amplified with primers 5'-CCCACTGAAAAAGATGAG-3' and 5'-CCTCCATGATGCTGCT-3', and used as a reference gene to normalize the amount and integrity of RNA. Mouse RNA was included in all experiments to rule out contamination by mouse RNA product.

Prognostic series of colorectal cancer patients

A cohort of 125 consecutive cases undergoing elective surgery between January 1996 and July 1997 was chosen to generate a tissue microarray (TMA). Prospective clinical follow-up was available for all patients. The main characteristics of the tumor series have been described previously (Landi et al., 2003; Moreno et al., 2006). Briefly, two tissue cylinders with diameters of 1.5 mm were punched from morphologically representative tissue areas of each donor tissue block and brought into one recipient paraffin block using an automated tissue arrayer. Four micron sections of the TMA blocks were transferred to an adhesive-coated slide system to facilitate the transfer of TMA sections to slides and to minimize tissue loss.

The TMA slides were deparaffinized with xylene and rehydrated through graded alcohols to water. Endogenous peroxidase activity was blocked with 3% hydrogen peroxidase for 10 min, followed by a 5-min wash in distilled water and three 5-min washes in phosphate-buffered saline (PBS). Antigen retrieval was obtained by boiling slides in a microwave oven (1200 W, 15 min) in 0.01 M citrate buffer pH 6.0. Nonspecific binding was blocked in a humidified chamber for 20 min in 10% normal goat serum. After washing with PBS, the sections were incubated with primary antibodies (PI4K2B rabbit polyclonal antibody, (Abcam, Ab37812) or STIM2 (anti-STIM2-CT sheep antibody provided by Lorna S. Johnstone (Williams et al., 2001)) in 1:50 dilution overnight at 4ºC. The sections were then incubated for 30 min with biotinylated link antibody and peroxidase-labeled streptavidin (DAKO K0675; Dako Diagnostics, Barcelona, Spain). Finally, the slides were incubated with diaminobenzidine chromogen solution and counterstained with hematoxylin. Positive and negative controls were included in each staining. Expression was evaluated according to the intensity (1 = -, undetectable or +, light; 2 = ++, moderate; 3 = +++, intense staining) and percentage of stain (1 = < 10 %; 2 = 10 - 50%; 3 = > 50% for PI4K2B; and 1 = 1 - 50%; 2 = > 50 - < 100%; 3 = 100% for STIM2). A score containing the information for both parameters [(intensity + 1) x percentage] was assigned. Two pathologists (N.B. and A.V.) blindly examined all slides. Agreement between the two observers was greater than 90%. Consensus was reached in the case of disagreement.

Adjuvant 5-FU-chemotherapy-treated colorectal cancer patient series

Between January 1996 and June 2000, a consecutive series of 214 colorectal cancer patients was identified undergoing elective radical surgery and treated adjuvantly with 5-FU. Paired fresh-frozen colorectal tumor and non-adjacent areas of normal colonic mucosa were simultaneously collected in 140 (65.4%) of the 214 patients. This group was used as the cohort used to study *PI4K2B* and *STIM2* gene expression levels by qPCR. Prospective clinical follow-up was available for all patients. The main characteristics of the tumor series have been described previously (Dotor et al., 2006). RNA was obtained from paired cases of normal colon mucosa and colorectal tumor using TRIZOL reagent following manufacturers' instructions (Invitrogen). Expression of *PI4K2B* and *STIM2* was assessed by qPCR (see above). Normalized expression ratios between matched primary tumors and normal colonic mucosa were calculated for *PI4K2B* and *STIM2*, and the median value was established as the cut-off. All reactions were performed independently in triplicate. The specific human *β_2-microglobulin* housekeeping gene was used for data normalization.

For both tumor series, overall survival (OS) and disease-free survival (DFS) were calculated from the time of surgery until

death, recurrence, or most recent follow-up visit. Written consent was obtained from all patients, and the hospital ethics committee approved the study protocol.

Silencing of *STIM2* or *PI4K2B* with small interference RNA (siRNA)

DLD-1 cells were transfected in 24-well plates using 1.0 µl of Lipofectamine 2000 and siRNAs at 100 nM concentration. To silence *PI4K2B* and *STIM2* mRNA, specific siRNAs were purchased from Ambion (AM51331 and AM16708A, respectively) and results were compared with those produced by the recommended negative control siRNA (AM4611). *PI4K2B* and *STIM2* protein levels were detected using rabbit polyclonal specific antibodies (Ab37812 and Ab59342, respectively) from Abcam in cell extracts 48 hours after siRNA transfection. Anti-ß-Actin-Peroxidase monoclonal antibody (A3854, Sigma) was used for loading control.

Proliferation [^{3}H]-thymidine incorporation assay

DLD-1 cells were seeded in a 24-well plate at 2500 cells per well. Cell growth was quantified 48 hours after transfection by incubation in DMEM (10% FBS) with 1 µCi/ml of [^{3}H]-thymidine (0.5 Ci/mmol, Amersham Biosciences) for 8 hours. Cells were rinsed with ice cold PBS, treated for 30 minutes at 4º C with ice cold 5% TCA solution, washed again with PBS, and dissolved with 500 µl of 0.5M NaOH at room temperature.

Transcriptional regulation analysis

The Pearson correlation coefficient (PCC) was used to examine expression correlations between *TCF4* microarray probes and probes in region A using the R programming language (www.r-project.org). For this analysis we used 295 primary colorectal carcinomas (CRCs) from the expO data set (Gene Expression Omnibus (GEO) reference GSE2109). Correlations in region A were compared to 10,000 random sets of 11 genes (with all their probes) from the same data set. The size of the random sets was chosen to reflect the number of known genes in region A and because the number of probes per gene varies. Direct transcriptional regulatory interactions for genes in region A were calculated with the ARACNe algorithm (Margolin et al., 2006) and using the expO data set. The *P* value threshold for mutual information (MI) significance was set to 1E-08 to reduce the number of estimated false positives to less than one. The data processing inequality (DPI) tolerance was set to 0.1 so that only 10% of the loops found in the network were kept, which ensured that only direct interactions were inferred. For both the correlation and the ARACNe analyses, the expO data set was previously normalized using the MAS5 algorithm implemented in the R Bioconductor suite, as this seems to be the normalization method that least overestimates the correlation between transcripts (Lim et al., 2007).

Chromatin immunoprecitation assay (ChIP)

The ChIP assay has been described previously (Aguilera et al., 2004). Briefly, chromatin from crosslinked cells was sonicated, incubated overnight with the indicated antibodies, α-ß-catenin (BD Bioscience 61054), in RIPA buffer, and precipitated with protein G/A-Sepharose. The antibodies used have been tested for the ChIP assay. Cross-linkage of the co-precipitated DNA-protein complexes was reversed, and DNA was purified and used as a template for semi-quantitative PCR.

Statistical analysis

Analysis of the expression data generated by qPCR was performed with the Relative Expression Software Tool (REST©) (Pfaffl et al., 2002), and the expression ratios were tested for significance using the Pair Wise Fixed Reallocation Randomization Test© and plotted using standard error (SE) estimation via a complex Taylor algorithm. P values for the clinicopathological features were calculated using the X^2 test. Survival curves were estimated using the Kaplan-Meier method, and differences between individual curves were evaluated by multivariate analyses using the Cox proportional hazards regression model. All analyses were adjusted for tumor stage, differentiation degree and tumor location. Hazard ratios (HRs) and 95% CIs were calculated. Likelihood ratio tests were used to assess the prognostic value of IHQ and quantitative RT-PCR expression levels. $P \leq 0.05$ was considered significant.

ACKNOWLEDGEMENTS

The authors would like to acknowledge the efforts of the International Genomics Consortium and the Expression Project for Oncology in making their expression data freely available (https://expo.intgen.org/geo/). AV, MN, AM and MA Pujana are researchers under the Ramón y Cajal program and LE is a researcher of Carlos III program. This study was supported by grants from the Spanish Ministry of Science and Technology (SAF2002-02265; SAF2006-06084; BFU2007-67123); Marató TV3 and the Fundación Mútua Madrileña. AA is a predoctoral fellow of the ISCIII and LP and MM-I of IDIBELL.

REFERENCES

1. Aguilera, C., Hoya-Arias, R., Haegeman, G., Espinosa, L., and Bigas, A. (2004). Recruitment of IkappaBalpha to the hes1 promoter is associated with transcriptional repression. Proceedings of the National Academy of Sciences of the United States of America *101*, 16537-16542.
2. Arribas, R., Ribas, M., Risques, R. A., Masramon, L., Tortola, S., Marcuello, E., Aiza, G., Miro, R., Capella, G., and Peinado, M. A. (1999a). Prospective assessment of allelic losses at 4p14-16 in colorectal cancer: two mutational patterns and a locus associated with poorer survival. Clin Cancer Res *5*, 3454-3459.
3. Arribas, R., Risques, R. A., Gonzalez-Garcia, I., Masramon, L., Aiza, G., Ribas, M., Capella, G., and Peinado, M. A. (1999b). Tracking recurrent quantitative genomic alterations in colorectal cancer: allelic losses in chromosome 4 correlate with tumor aggressiveness. Lab Invest *79*, 111-122.
4. Bardi, G., Fenger, C., Johansson, B., Mitelman, F., and Heim, S. (2004). Tumor karyotype predicts clinical outcome in colorectal cancer patients. J Clin Oncol *22*, 2623-2634.
5. Berridge, M. J. (1987). Inositol trisphosphate and diacylglycerol: two interacting second messengers. Annu Rev Biochem *56*, 159-193.
6. Brandman, O., Liou, J., Park, W. S., and Meyer, T. (2007). STIM2 is a feedback regulator that stabilizes basal cytosolic and endoplasmic reticulum Ca2+ levels. Cell *131*, 1327-1339.
7. Caldas, C., Hahn, S. A., da Costa, L. T., Redston, M. S., Schutte, M., Seymour, A. B., Weinstein, C. L., Hruban, R. H., Yeo, C. J., and Kern, S. E. (1994). Frequent somatic mutations and homozygous deletions of the p16 (MTS1) gene in pancreatic adenocarcinoma. Nat Genet *8*, 27-32.
8. Cappione, A. J., French, B. L., and Skuse, G. R. (1997). A potential role for NF1 mRNA editing in the pathogenesis of NF1 tumors. American journal of human genetics *60*, 305-312.
9. Cavenee, W. K., Hansen, M. F., Nordenskjold, M., Kock, E., Maumenee, I., Squire, J. A., Phillips, R. A., and Gallie, B. L. (1985). Genetic origin of mutations predisposing to retinoblastoma. Science (New York, NY *228*, 501-503.
10. Deans, G. T., Parks, T. G., Rowlands, B. J., and Spence, R. A. (1992). Prognostic factors in colorectal cancer. Br J Surg *79*, 608-613.
11. Diep, C. B., Kleivi, K., Ribeiro, F. R., Teixeira, M. R., Lindgjaerde, O. C., and Lothe, R. A. (2006). The order of genetic events associated with colorectal cancer progression inferred from meta-analysis of copy number changes. Genes Chromosomes Cancer *45*, 31-41.
12. Dotor, E., Cuatrecases, M., Martinez-Iniesta, M., Navarro, M., Vilardell, F., Guino, E., Pareja, L., Figueras, A., Mollevi, D. G., Serrano, T., *et al.* (2006). Tumor thymidylate synthase 1494del6 genotype as a prognostic factor in colorectal cancer patients receiving fluorouracil-based adjuvant treatment. J Clin Oncol *24*, 1603-1611.
13. Dutrillaux, B., Gerbault-Seureau, M., Remvikos, Y., Zafrani, B., and Prieur, M. (1991). Breast cancer genetic evolution: I. Data from cytogenetics and DNA content. Breast Cancer Res Treat *19*, 245-255.
14. Fearon, E. R., and Vogelstein, B. (1990). A genetic model for colorectal tumorigenesis. Cell *61*, 759-767.
15. Frigola, J., Song, J., Stirzaker, C., Hinshelwood, R. A., Peinado, M. A., and Clark, S. J. (2006). Epigenetic remodeling in colorectal cancer results in coordinate gene suppression across an entire chromosome band. Nat Genet *38*, 540-549.
16. Fruman, D. A., Meyers, R. E., and Cantley, L. C. (1998). Phosphoinositide kinases. Annu Rev Biochem *67*, 481-507.
17. Grade, M., Becker, H., Liersch, T., Ried, T., and Ghadimi, B. M. (2006). Molecular cytogenetics: genomic imbalances in colorectal cancer and their clinical impact. Cell Oncol *28*, 71-84.
18. Landi, S., Moreno, V., Gioia-Patricola, L., Guino, E., Navarro, M., de Oca, J., Capella, G., and Canzian, F. (2003). Association of common polymorphisms in inflammatory genes interleukin (IL)6, IL8, tumor necrosis factor alpha, NFKB1, and peroxisome proliferator-activated receptor gamma with colorectal cancer. Cancer research *63*, 3560-3566.

19. Lim, W. K., Wang, K., Lefebvre, C., and Califano, A. (2007). Comparative analysis of microarray normalization procedures: effects on reverse engineering gene networks. Bioinformatics *23*, i282-288.
20. Liou, J., Kim, M. L., Heo, W. D., Jones, J. T., Myers, J. W., Ferrell, J. E., Jr., and Meyer, T. (2005). STIM is a Ca2+ sensor essential for Ca2+-store-depletion-triggered Ca2+ influx. Curr Biol 15, 1235-1241.
21. Malkhosyan, S., Yasuda, J., Soto, J. L., Sekiya, T., Yokota, J., and Perucho, M. (1998). Molecular karyotype (amplotype) of metastatic colorectal cancer by unbiased arbitrarily primed PCR DNA fingerprinting. Proceedings of the National Academy of Sciences of the United States of America *95*, 10170-10175.
22. Margolin, A. A., Nemenman, I., Basso, K., Wiggins, C., Stolovitzky, G., Dalla Favera, R., and Califano, A. (2006). ARACNE: an algorithm for the reconstruction of gene regulatory networks in a mammalian cellular context. BMC Bioinformatics *7 Suppl 1*, S7.
23. Moreno, V., Gemignani, F., Landi, S., Gioia-Patricola, L., Chabrier, A., Blanco, I., Gonzalez, S., Guino, E., Capella, G., and Canzian, F. (2006). Polymorphisms in genes of nucleotide and base excision repair: risk and prognosis of colorectal cancer. Clin Cancer Res *12*, 2101-2108.
24. Nadal, M., Moreno, S., Pritchard, M., Preciado, M. A., Estivill, X., and Ramos-Arroyo, M. A. (1997). Down syndrome: characterisation of a case with partial trisomy of chromosome 21 owing to a paternal balanced translocation (15;21) (q26;q22.1) by FISH. J Med Genet *34*, 50-54.
25. Nishizuka, Y. (1984). The role of protein kinase C in cell surface signal transduction and tumour promotion. Nature *308*, 693-698.
26. Parkin, D. M., Pisani, P., and Ferlay, J. (1993). Estimates of the worldwide incidence of eighteen major cancers in 1985. Int J Cancer *54*, 594-606.
27. Parvez, S., Beck, A., Peinelt, C., Soboloff, J., Lis, A., Monteilh-Zoller, M., Gill, D. L., Fleig, A., and Penner, R. (2008). STIM2 protein mediates distinct store-dependent and store-independent modes of CRAC channel activation. Faseb J *22*, 752-761.
28. Pershouse, M. A., El-Naggar, A. K., Hurr, K., Lin, H., Yung, W. K., and Steck, P. A. (1997a). Deletion mapping of chromosome 4 in head and neck squamous cell carcinoma. Oncogene *14*, 369-373.
29. Pershouse, M. A., Ligon, A. H., Pereira-Smith, O. M., Killary, A. M., Yung, W. K., and Steck, P. A. (1997b). Suppression of transformed phenotype and tumorigenicity after transfer of chromosome 4 into U251 human glioma cells. Genes Chromosomes Cancer *20*, 260-267.
30. Pfaffl, M. W., Horgan, G. W., and Dempfle, L. (2002). Relative expression software tool (REST) for group-wise comparison and statistical analysis of relative expression results in real-time PCR. Nucleic Acids Res *30*, e36.
31. Piao, Z., Park, C., Park, J. H., and Kim, H. (1998). Deletion mapping of chromosome 4q in hepatocellular carcinoma. Int J Cancer *79*, 356-360.
32. Polascik, T. J., Cairns, P., Chang, W. Y., Schoenberg, M. P., and Sidransky, D. (1995). Distinct regions of allelic loss on chromosome 4 in human primary bladder carcinoma. Cancer research *55*, 5396-5399.
33. Reya, T., and Clevers, H. (2005). Wnt signalling in stem cells and cancer. Nature *434*, 843-850.
34. Ruano, Y., Mollejo, M., Ribalta, T., Fiano, C., Camacho, F. I., Gomez, E., de Lope, A. R., Hernandez-Moneo, J. L., Martinez, P., and Melendez, B. (2006). Identification of novel candidate target genes in amplicons of Glioblastoma multiforme tumors detected by expression and CGH microarray profiling. Mol Cancer *5*, 39.
35. Sabbioni, S., Barbanti-Brodano, G., Croce, C. M., and Negrini, M. (1997). GOK: a gene at 11p15 involved in rhabdomyosarcoma and rhabdoid tumor development. Cancer research *57*, 4493-4497.
36. Sabbioni, S., Veronese, A., Trubia, M., Taramelli, R., Barbanti-Brodano, G., Croce, C. M., and Negrini, M. (1999). Exon structure and promoter identification of STIM1 (alias GOK), a human gene causing growth arrest of the human tumor cell lines G401 and RD. Cytogenet Cell Genet *86*, 214-218.
37. Sherwood, J. B., Shivapurkar, N., Lin, W. M., Ashfaq, R., Miller, D. S., Gazdar, A. F., and Muller, C. Y. (2000). Chromosome 4 deletions are frequent in invasive cervical cancer and differ between histologic variants. Gynecol Oncol *79*, 90-96.
38. Shiotsuka, S., and Isonishi, S. (2001). Differential sensitization by orobol in proliferating and quiescent human ovarian carcinoma cells. International journal of oncology *18*, 337-342.
39. Shivapurkar, N., Maitra, A., Milchgrub, S., and Gazdar, A. F. (2001). Deletions of chromosome 4 occur early during the pathogenesis of colorectal carcinoma. Human pathology *32*, 169-177.
40. Shivapurkar, N., Sood, S., Wistuba, II, Virmani, A. K., Maitra, A., Milchgrub, S., Minna, J. D., and Gazdar, A. F. (1999). Multiple regions of chromosome 4 demonstrating allelic losses in breast carcinomas. Cancer research *59*, 3576-3580.
41. Sjoblom, T., Jones, S., Wood, L. D., Parsons, D. W., Lin, J., Barber, T. D., Mandelker, D., Leary, R. J., Ptak, J., Silliman, N., *et al.* (2006). The consensus coding sequences of human breast and colorectal cancers. Science (New York, NY *314*, 268-274.
42. Soboloff, J., Spassova, M. A., Hewavitharana, T., He, L. P., Xu, W., Johnstone, L. S., Dziadek, M. A., and Gill, D.

L. (2006). STIM2 is an inhibitor of STIM1-mediated store-operated Ca2+ Entry. Curr Biol *16*, 1465-1470.
43. Stanbridge, E. J. (1990). Identifying tumor suppressor genes in human colorectal cancer. Science (New York, NY *247*, 12-13.
44. Suyama, E., Wadhwa, R., Kaur, K., Miyagishi, M., Kaul, S. C., Kawasaki, H., and Taira, K. (2004). Identification of metastasis-related genes in a mouse model using a library of randomized ribozymes. J Biol Chem *279*, 38083-38086.
45. Tarafa, G., Villanueva, A., Farre, L., Rodriguez, J., Musulen, E., Reyes, G., Seminago, R., Olmedo, E., Paules, A. B., Peinado, M. A., *et al*. (2000). DCC and SMAD4 alterations in human colorectal and pancreatic tumor dissemination. Oncogene *19*, 546-555.
46. Thiagalingam, S., Laken, S., Willson, J. K., Markowitz, S. D., Kinzler, K. W., Vogelstein, B., and Lengauer, C. (2001). Mechanisms underlying losses of heterozygosity in human colorectal cancers. Proceedings of the National Academy of Sciences of the United States of America *98*, 2698-2702.
47. Tomlinson, I. P., Lambros, M. B., and Roylance, R. R. (2002). Loss of heterozygosity analysis: practically and conceptually flawed? Genes Chromosomes Cancer *34*, 349-353.
48. Williams, R. T., Manji, S. S., Parker, N. J., Hancock, M. S., Van Stekelenburg, L., Eid, J. P., Senior, P. V., Kazenwadel, J. S., Shandala, T., Saint, R., *et al*. (2001). Identification and characterization of the STIM (stromal interaction molecule) gene family: coding for a novel class of transmembrane proteins. Biochem J *357*, 673-685.

FIGURE LEGENDS

Figure 1 LOH patterns at 4p14-16. **(A)** LOH status of thirty microsatellites in 24 matched cases of normal mucosa/CRC/CRC-X. A complex profile of LOH for the 4p14-16 region is depicted, although it is difficult to define a small common minimal region of loss. A range of 1-6 discrete areas of loss was defined. CRC8 only lost the D4S2397 marker. One subregion is defined in CRC28, two in CRC25 and CRC26, three in CRC16 and CRC24, four in CRC4, five in CRC19 and six in CRC9B and CRC11 tumors, respectively. **(B)** LOH for hepatic metastasis for the thirty microsatellites studied in CRC. A total region of 32 Mbp, which represents 64% of the short arm (4p) of chromosome 4, was analyzed in twenty matched cases of normal hepatic parenchyma/HM/HM-X. A further 27 telomeric markers (in red) flanked by D4S3360 and D4S2946 were analyzed in HM. The region is lost in HM12 and HM20, while two areas can be defined in HM3 and HM15, and three in HM10. **(C)** LOH status for distal metastases obtained during *in vivo* distal dissemination in nude mice. A subset of twelve representative microsatellite markers were analyzed in matched cases of normal mucosa—CRC—nude mice metastases.
*, Two independent tumors or hepatic metastases were obtained from the same patient.
#1 to #4. Number of peritoneal implants analyzed.

Figure 2 Integrative genomic approach for region A gene analysis. **(A)** Left panel, transcript profile correlations in a series of 295 CRCs between genes in region A (bottom, probes are not shown) and *TCF4* probes, measured by PCC. Right panel, distribution of average absolute PCCs for sets of 11 genes randomly chosen from the same series (blue curve) and for the genes in region A (vertical dashed red line). Arrows indicate the values of the two top absolute correlations of single probes in region A. **(B)** Predicted direct transcriptional regulatory interactions for genes in region A in the same series of CRCs. Predicted targets and regulators (transcription factors) are shown as indicated in the inset. **(C)** Experimental verification of regulatory predictions of *PI4K2B* and *STIM2* by chromatin immunoprecipitation (Chip) in non-CRC and CRC cell lines using a β-catenin antibody and the corresponding controls as shown (inputs and irrelevant IgG; see *Methods*).

Figure 3 Determination of mRNA expression levels in colorectal tumors by qPCR. **(A)** Normalized qPCR expression results for human *STIM2*, *PI4K2B*, *KIAA0746*, *RBPSUH* and *ANAPC4* genes. Analysis was assessed in ten colorectal tumor xenografts with LOH for the 4p14-16 region (upper panel), and in ten other tumors without LOH (lower panel). **(B)** *STIM2* and *PI4K2B* expression in twenty cases of matched normal mucosa and tumor xenograft samples. Results are distributed according to LOH status. Arrows indicate expression for two different tumors obtained from the same patient with different LOH status. **(C)** Box-plots

comparing *STIM2* and *PI4K2B* and expression between normal colon mucosa and colorectal tumors. Significant differences for all tumors, or classified according to LOH status. **(D)** Normalized qPCR expression results for the five genes assessed in five xenografted colorectal hepatic metastases (left panel) with LOH for the 4p14-16 region, and in a further five without LOH. Right panel, box-plots for *STIM2* (upper panel) and *PI4K2B* (lower panel) expression levels between HM and a pool of normal colon mucosa. Normalization of RNA was assessed by the human β_2-*microglobulin* housekeeping gene. Experiments were performed in triplicate. In all experiments, mouse RNA was included to rule out contamination by mouse RNA products. $P < 0.05$ was considered significant.

Figure 4 Interphase fluorescence *in situ* hybridization (FISH) analysis in tumor touch imprints. FISH and LOH results are shown for the same tumor sample. Four different fluorescent probes located along the 4p short arm were used to assess the complete or partial loss of the short arm of chromosome 4. RP11-372F2 (4p16.3, close to the telomere), RP11-293A21 (4p15.2, containing the STIM2 gene), RP11-473F10 (4p, containing the PI4K2B gene) and RP11-475J10 (4p13, close to the centromere) were hybridized in pairs [RP11-372F2 with RP11-293A21; RP11-473F10 with RP11-475J10]. A total of 100 non-overlapping nuclei showing clear signals were scored for hybridization. **(A)** Map of probe location; **(B)** Representative FISH analysis of RP11-372F2/RP11-293A21 (left panel) and RP11-473F10/RP11-475J10 (right panel) in CRC24 tumor xenograft shows LOH by microsatellite markers and is diploid by FISH analysis; **(C)** FISH results of RP11-473F10/RP11-475J10 in tumor xenografts of CRC19, CRC28 and HM12, all showing LOH by microsatellite analysis. CRC19 harbors a deletion at 4p, revealed by FISH. CRC28 shows a deletion, while HM12 shows a clear triploidy.

Figure 5 Prognostic value of PI4K2B and STIM2 expression levels. **(A)** Representative IHQ staining for PI4K2B (upper panel) and STIM2 (lower panel). **(B)** IHQ Kaplan-Meier plots for PI4K2B. Overall survival (OS) according to staining intensity (low intensity: - or +; high intensity: ++ or +++) (upper panel); and OS (middle panel) and disease-free survival (DFS) (lower panel) in terms of an IHQ expression score combining intensity and percentage of cell staining parameters (low score: [2, 5]; high score: [5, 12]). P values correspond to multivariate Cox proportional hazards regression models adjusted for the Dukes staging system. **(C)** *PI4K2B* mRNA expression levels determined by qPCR in a series of colorectal tumors homogeneously treated with 5-FU. OS (upper panel) and DFS (lower panel) for patients defined as of High and Low *PI4K2B* mRNA expression using the median value of the tumor/normal ratio as a cut-off. P values correspond to multivariate Cox proportional hazards regression models adjusted for the Dukes staging system.

Figure 6 siRNA-mediated silencing of *PI4K2B* or *STIM2* increases cell growth in DLD-1 colorectal tumor cells. **(A)** qPCR levels of *PI4K2B* or *STIM2* in colorectal cancer cell lines. **(B)** DLD-1 cells were transfected with STIM2 and control siRNA, and protein levels were measured after 48 hours by western blot. ß-Actin was used as a loading control. A representative image of three independent experiments and their quantification are shown. $n = 2$, *$p < 0.01$. **(C)** Cell growth was determined 48 hours after transfection of STIM2 and control siRNA-treated DLD-1 cells by analyzing [^{3}H]-thymidine incorporation. $n = 3$, *$p < 0.01$. C, PI4K2B levels from PI4KB and control siRNA transfected cells were detected by western blot and quantified using Quantity One software (Biorad). ß-Actin was used as a loading control. $n = 2$, *$p < 0.01$. D, [^{3}H]-thymidine incorporation (8 hours) was measured in DLD-1 cells transfected with PI4KB siRNA or control siRNA. $n = 3$, *$p < 0.01$.

Figure 1

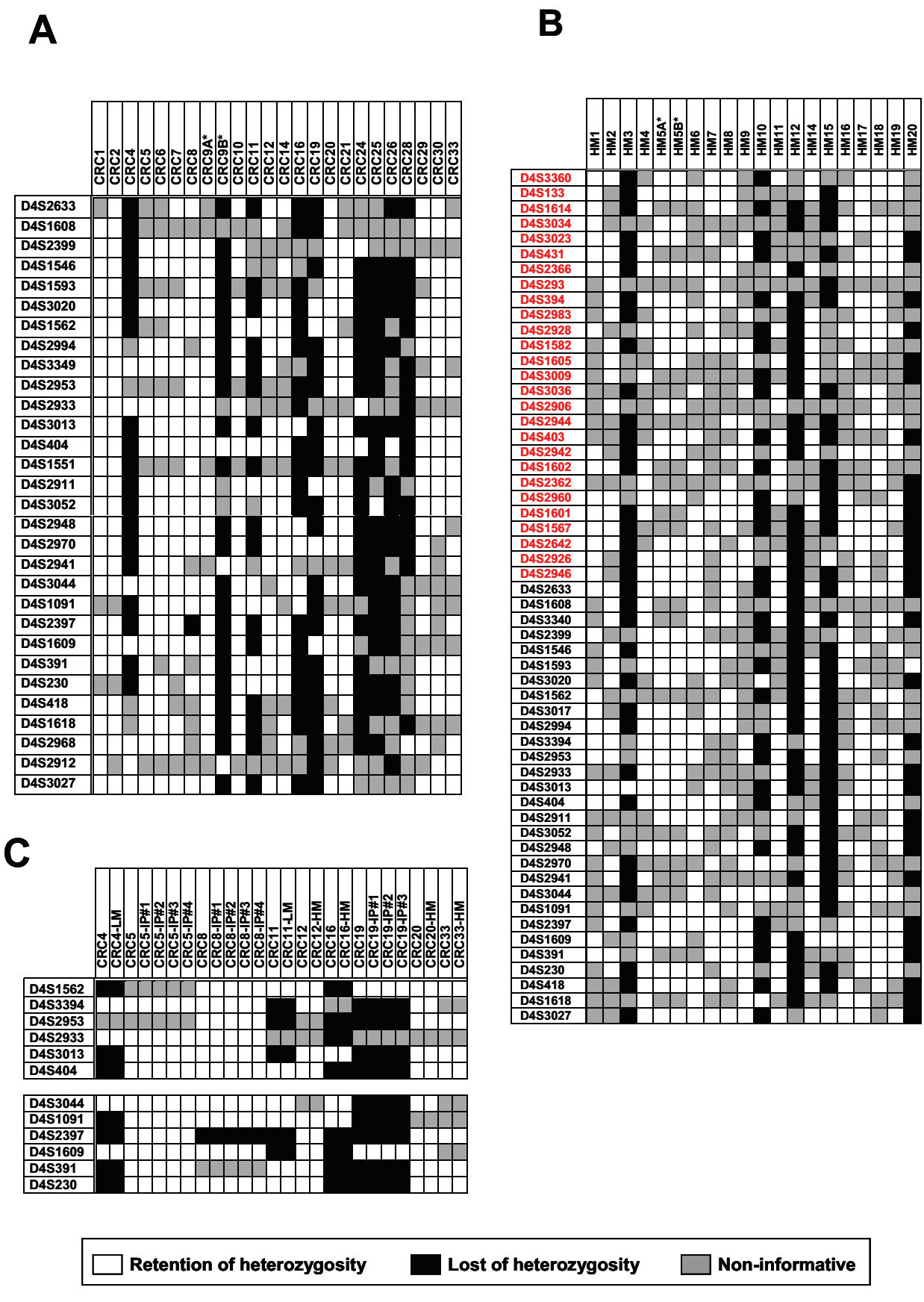
A
CRC1
CRC2
CRC4
CRC5
CRC6
CRC7
CRC8
CRC9A*
CRC9B*
CRC10
CRC11
CRC12
CRC14
CRC16
CRC19
CRC20
CRC21
CRC24
CRC25
CRC26
CRC28
CRC29
CRC30
CRC33
D4S2633
D4S1608
D4S2399
D4S1546
D4S1593
D4S3020
D4S1562
D4S2994
D4S3349
D4S2953
D4S2933
D4S3013
D4S404
D4S1551
D4S2911
D4S3052
D4S2948
D4S2970
D4S2941
D4S3044
D4S1091
D4S2397
D4S1609
D4S391
D4S230
D4S418
D4S1618
D4S2968
D4S2912
D4S3027
B
HM1
HM2
HM3
HM4
HM5A*
HM5B*
HM6
HM7
HM8
HM9
HM10
HM11
HM12
HM14
HM15
HM16
HM17
HM18
HM19
HM20
D4S3360
D4S133
D4S1614
D4S3034
D4S3023
D4S431
D4S2366
D4S293
D4S394
D4S2983
D4S2928
D4S1582
D4S1605
D4S3009
D4S3036
D4S2906
D4S2944
D4S403
D4S2942
D4S1602
D4S2362
D4S2960
D4S1601
D4S1567
D4S2642
D4S2926
D4S2946
D4S2633
D4S1608
D4S3340
D4S2399
D4S1546
D4S1593
D4S3020
D4S1562
D4S3017
D4S2994
D4S3394
D4S2953
D4S2933
D4S3013
D4S404
D4S2911
D4S3052
D4S2948
D4S2970
D4S2941
D4S3044
D4S1091
D4S2397
D4S1609
D4S391
D4S230
D4S418
D4S1618
D4S3027
C
CRC4
CRC4-LM
CRC5
CRC5-IP#1
CRC5-IP#2
CRC5-IP#3
CRC5-IP#4
CRC8
CRC8-IP#1
CRC8-IP#2
CRC8-IP#3
CRC8-IP#4
CRC11
CRC11-LM
CRC12
CRC12-HM
CRC16
CRC16-HM
CRC19
CRC19-IP#1
CRC19-IP#2
CRC19-IP#3
CRC20
CRC20-HM
CRC33
CRC33-HM
D4S1562
D4S3394
D4S2953
D4S2933
D4S3013
D4S404
D4S3044
D4S1091
D4S2397
D4S1609
D4S391
D4S230
Retention of heterozygosity
Lost of heterozygosity
Non-informative

Figure 2

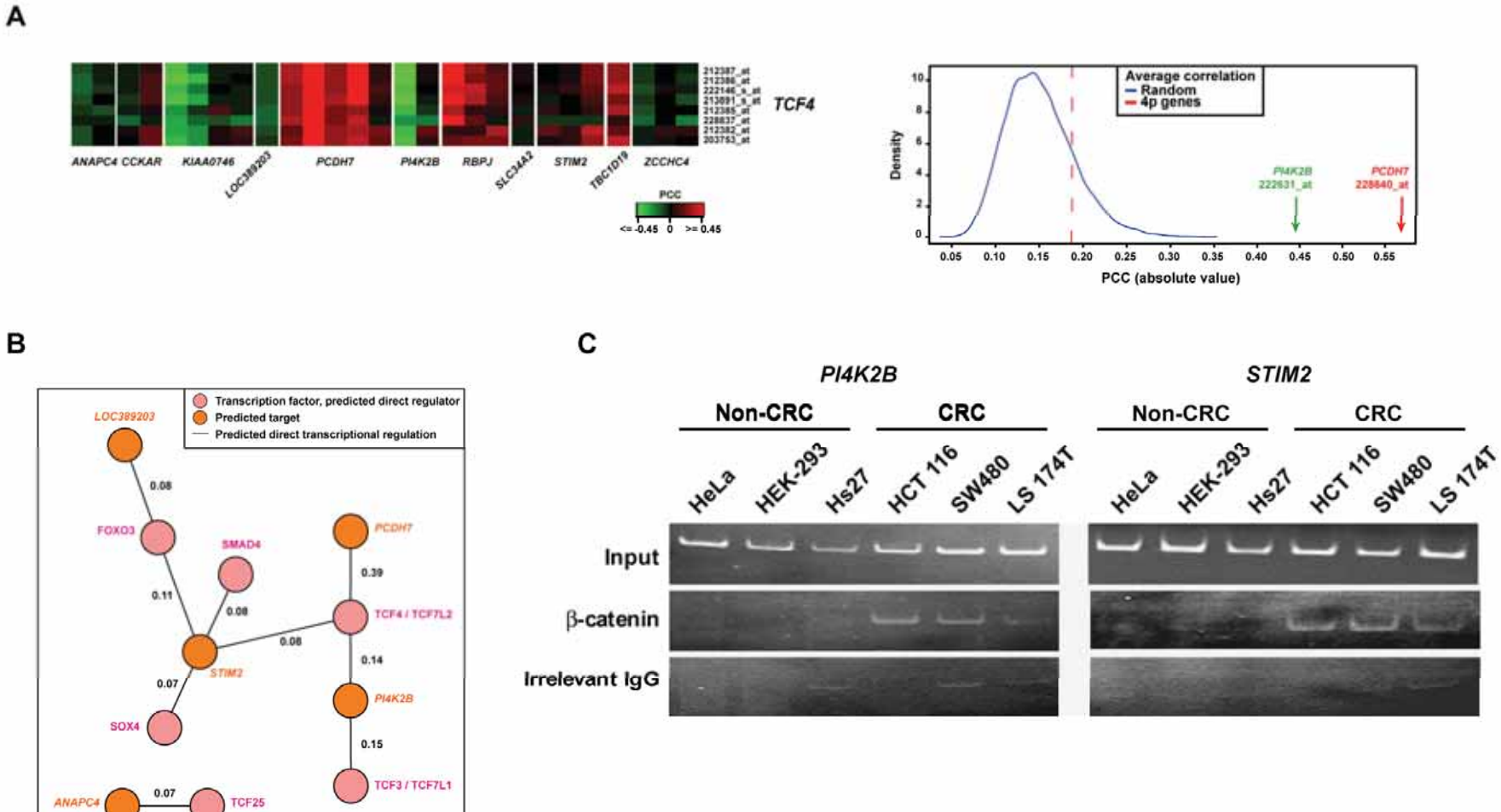
A
ANAPC4
CCKAR
KIAA0746
LOC389203
PCDH7
PI4K2B
RBPJ
SLC34A2
STIM2
TBC1D19
ZCCHC4
TCF4
PCC
<= -0.45 0 >= 0.45
Average correlation
Random
4p genes
Density
PI4K2B
222631_at
PCDH7
228640_at
PCC (absolute value)
B
Transcription factor, predicted direct regulator
Predicted target
Predicted direct transcriptional regulation
LOC389203
FOXO3
SMAD4
PCDH7
TCF4 / TCF7L2
STIM2
PI4K2B
SOX4
TCF3 / TCF7L1
ANAPC4
TCF25
C
PI4K2B
STIM2
Non-CRC
CRC
HeLa
HEK-293
Hs27
HCT 116
SW480
LS 174T
Input
β-catenin
Irrelevant IgG

Figure 3

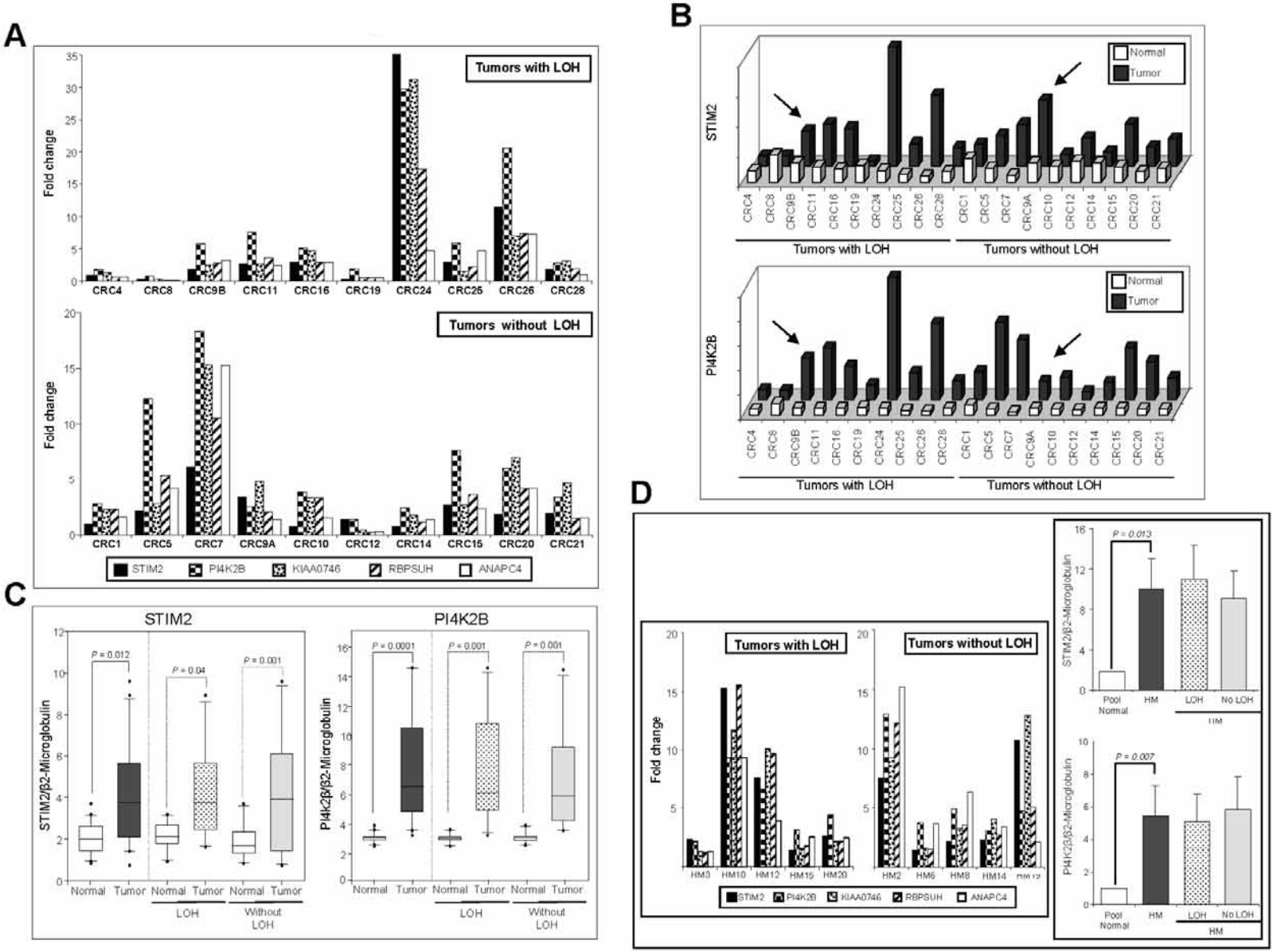
A
Tumors with LOH
Fold change
CRC4 CRC8 CRC9B CRC11 CRC16 CRC19 CRC24 CRC25 CRC26 CRC28
Tumors without LOH
CRC1 CRC5 CRC7 CRC9A CRC10 CRC12 CRC14 CRC15 CRC20 CRC21
STIM2 PI4K2B KIAA0746 RBPSUH ANAPC4
B
Normal
Tumor
STIM2
PI4K2B
Tumors with LOH
Tumors without LOH
C
STIM2
PI4K2B
STIM2/β2-Microglobulin
PI4K2β/β2-Microglobulin
P = 0.012
P = 0.04
P = 0.001
P = 0.0001
Normal Tumor
LOH
Without LOH
D
Tumors with LOH
Tumors without LOH
Fold change
HM3 HM10 HM12 HM15 HM20
HM2 HM6 HM8 HM14
STIM2 PI4K2B KIAA0746 RBPSUH ANAPC4
P = 0.013
P = 0.007
STIM2/β2-Microglobulin
PI4K2β/β2-Microglobulin
Pool Normal
HM
LOH
No LOH

Figure 4

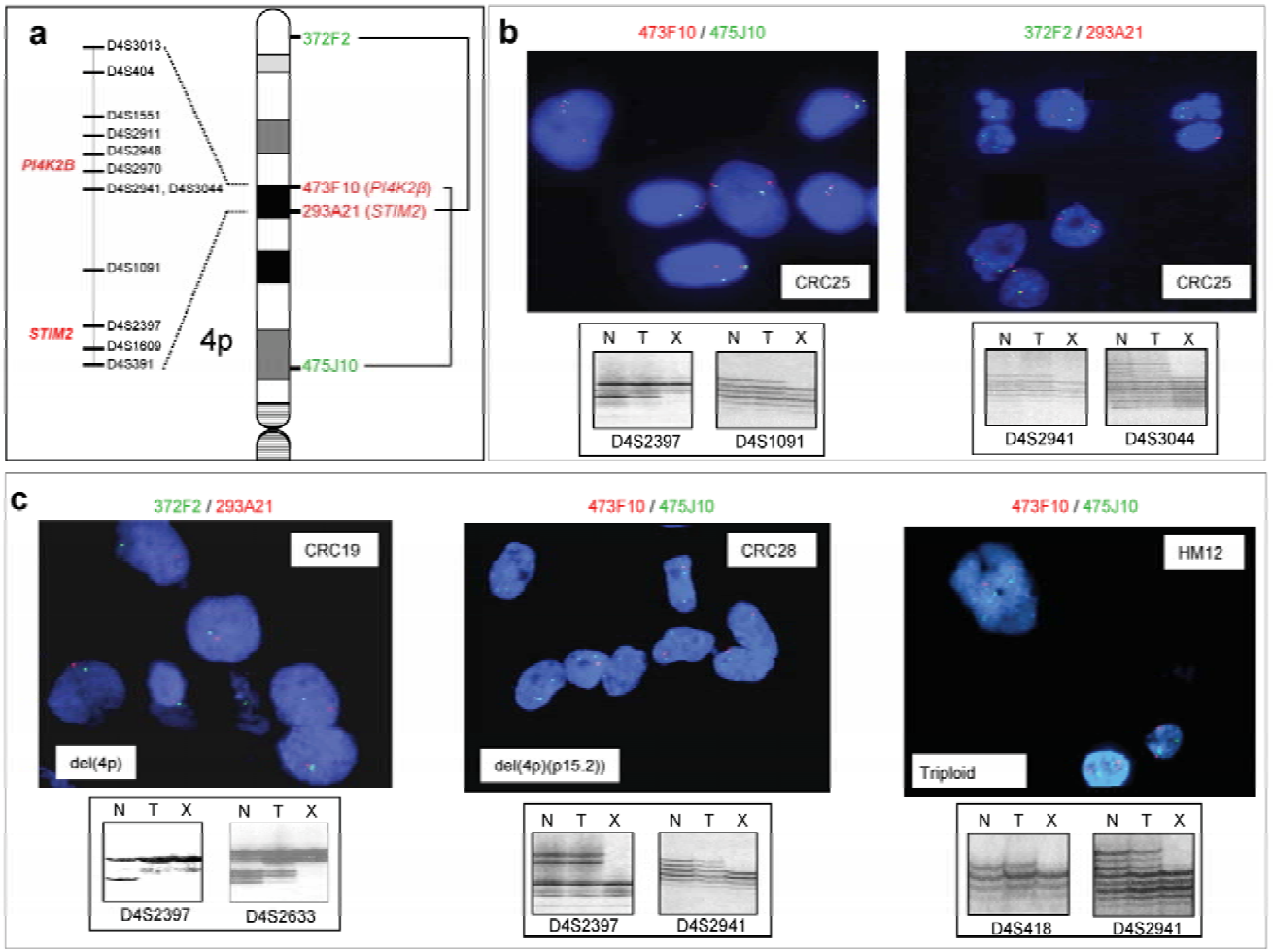
a
D4S3013
D4S404
D4S1551
D4S2911
D4S2948
PI4K2B
D4S2970
D4S2941, D4S3044
D4S1091
STIM2
D4S2397
D4S1609
D4S391
4p
372F2
473F10 (PI4K2β)
293A21 (STIM2)
475J10
b
473F10 / 475J10
CRC25
N T X N T X
D4S2397 D4S1091
372F2 / 293A21
CRC25
N T X N T X
D4S2941 D4S3044
c
372F2 / 293A21
CRC19
del(4p)
N T X N T X
D4S2397 D4S2633
473F10 / 475J10
CRC28
del(4p)(p15.2))
N T X N T X
D4S2397 D4S2941
473F10 / 475J10
HM12
Triploid
N T X N T X
D4S418 D4S2941

Figure 5

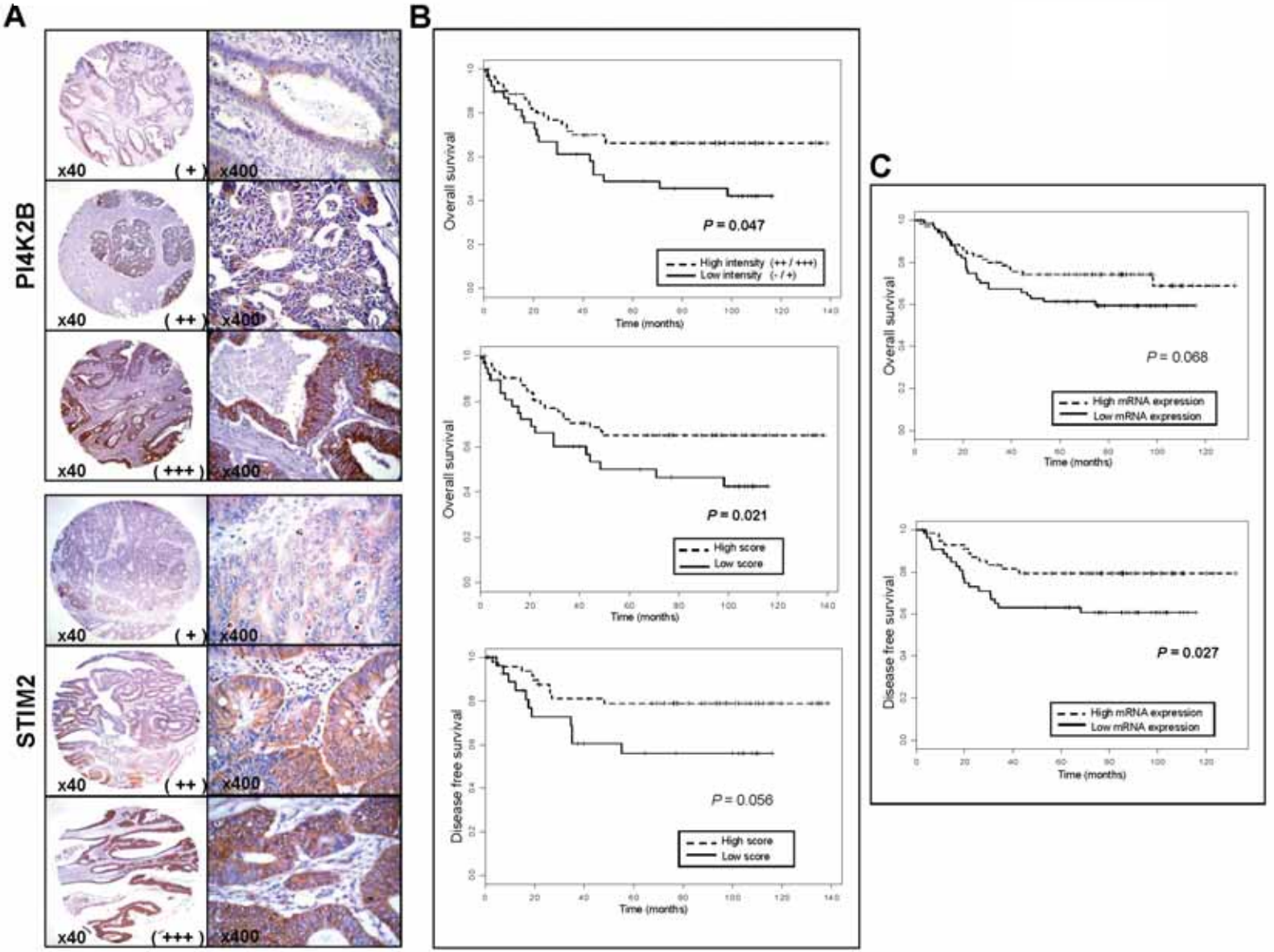
A
PI4K2B
x40
(+)
x400
x40
(++)
x400
x40
(+++)
x400
STIM2
x40
(+)
x400
x40
(++)
x400
x40
(+++)
x400
B
Overall survival
P = 0.047
High intensity (++ / +++)
Low intensity (- / +)
Time (months)
Overall survival
P = 0.021
High score
Low score
Time (months)
Disease free survival
P = 0.056
High score
Low score
Time (months)
C
Overall survival
P = 0.068
High mRNA expression
Low mRNA expression
Time (months)
Disease free survival
P = 0.027
High mRNA expression
Low mRNA expression
Time (months)

Figure 6

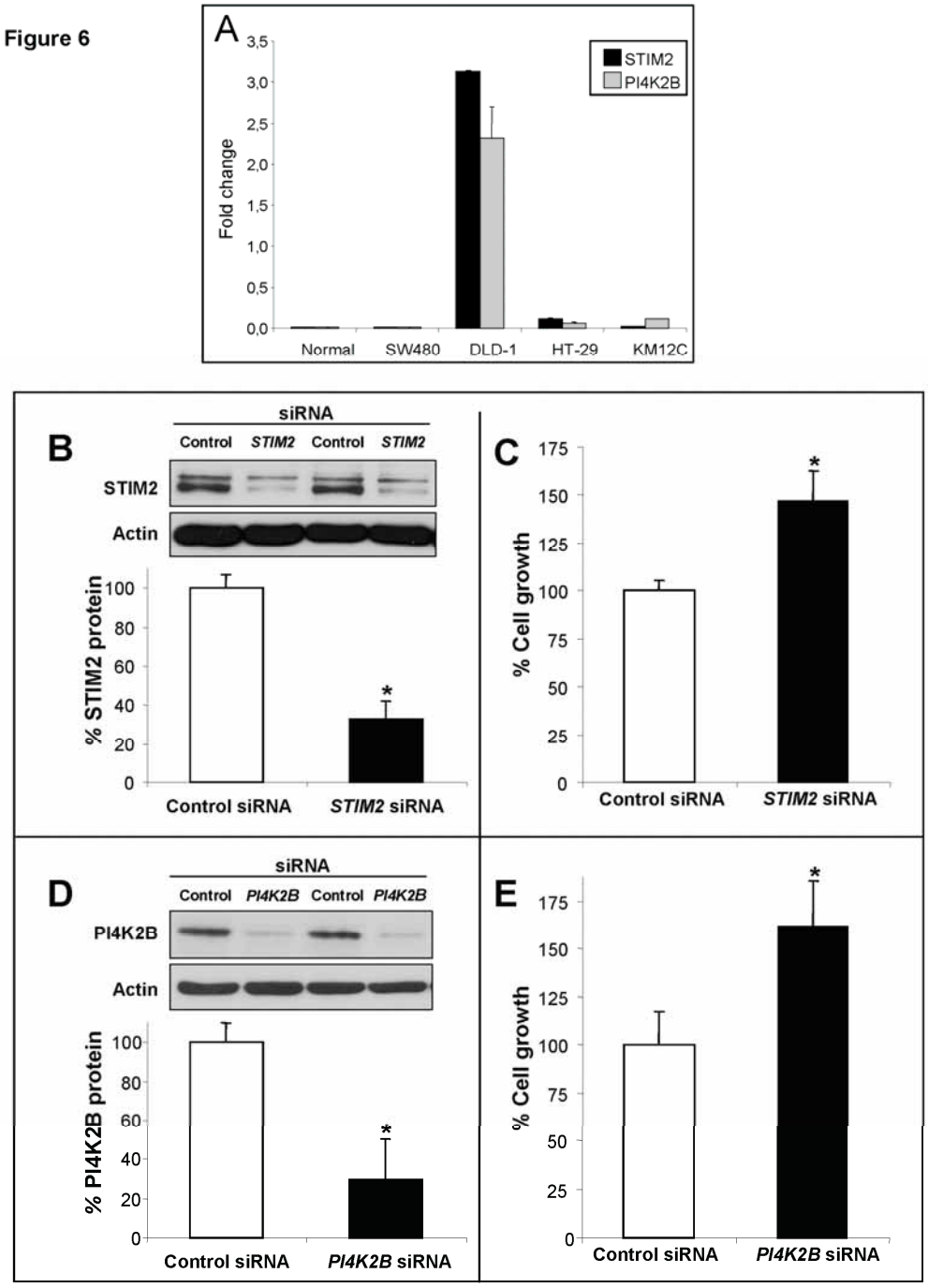
Figure 6
A
Fold change
3,5
3,0
2,5
2,0
1,5
1,0
0,5
0,0
STIM2
PI4K2B
Normal
SW480
DLD-1
HT-29
KM12C
B
siRNA
Control
STIM2
Control
STIM2
STIM2
Actin
% STIM2 protein
100
80
60
40
20
0
Control siRNA
STIM2 siRNA
C
% Cell growth
175
150
125
100
75
50
25
0
Control siRNA
STIM2 siRNA
D
siRNA
Control
PI4K2B
Control
PI4K2B
PI4K2B
Actin
% PI4K2B protein
100
80
60
40
20
0
Control siRNA
PI4K2B siRNA
E
% Cell growth
175
150
125
100
75
50
25
0
Control siRNA
PI4K2B siRNA

Table 1 Immunohistochemical analysis of PI4K2B and STIM2 expression.

	Overall Survival (OS)					Disease-Free Survival (DFS)				
PI4K2B	**No**	**%**	**HR**	**95% CI**	***P*§**	**No**	**%**	**HR**	**95% CI**	P§
Staining Intensity*										
++ or +++	61	60.4	1			50	61.7	1		
- or +	40	39.6	1.89	(1.01 – 3.52)	**0.047**	31	38.3	2.31	(0.98 – 5.44)	**0.058**
Tumor cells expression PI4K2B†										
>10%	84	83.2	1			67	82.7	1		
≤10%	17	17.8	1.29	(0.59 – 2.83)	0.533	14	16.3	1.54	(0.56 – 4.27)	0.424
PI4K2B Score (I:P)‡										
High	62	61.4	1			50	61.7	1		
Low	39	38.6	2.12	(1.13 – 3.97)	**0.021**	31	38.3	2.32	(0.98 – 5.5)	**0.056**
STIM2										
Staining Intensity*										
++ or +++	74	65.5	1			65	69.1	1		
- or +	39	34.5	0.93	(0.5 – 1.72)	0.817	29	30.9	0.75	(0.32 – 1.78)	0.508
Tumor cells expression STIM2†										
100%	97	85.8	1			81	86.2	1		
<100%	16	14.1	0.67	(0.28 – 1.6)	0.346	13	13.8	0.96	(0.33 – 2.79)	0.937
STIM2 Score (I:P)‡										
High	68	60.2	1			59	62.8	1		
Low	45	39.8	0.93	(0.51 – 1.69)	0.808	35	37.2	0.81	(0.36 – 1.8)	0.602

Abbreviations: HR, hazard ratio; CI, confidence interval; I, intensity; P, percentage

*staining intensity: - = undetectable; + = trace of staining; ++ = definite staining of light to moderate intensity; +++ = High intensity of staining

† Percentage of tumor cells expressing PI4K2B (≤10% or >10%) and STIM2 (100% or <100%).

‡ Score of PI4K2B or STIM2 considering intensity and percentage [(I + 1) x P] and grouping in Low or High score value

P values correspond to Cox proportional hazards regression models adjusted for tumor stage.

Table 2 Quantitative real-time PCR (qPCR) analysis of *PI4K2B* and *STIM2* mRNA expression levels in 5-FU-adjuvant treated colorectal cancer patients.

	Overall Survival (OS)					Disease-Free Survival (DFS)				
Expression levels	**No**	**%**	**HR**	**95% CI**	***P****	**No**	**%**	**HR**	**95% CI**	***P****
***PI4K2B*†**										
High Expression	70	50	1			55	50.5	1		
Low expression	70	50	1.72	(0.95 – 3.1)	0.068	54	49.5	2.25	(1.07 – 4.7)	**0.027**
***STIM2*†**										
High Expression	70	50	1			61	56	1		
Low expression	70	50	1.02	(0.55 – 1.9)	0.94	48	44	0.84	(0.41 – 1.74)	0.64
Synergistic models										
Additive model‡										
PI4K2B and *STIM2* up-regulated	52	37.1	1			46	42.2	1		
One or both down-regulated	88	62.9	1.57	(0.8 – 3.07)	0.19	63	57.8	1.79	(0.84 – 3.8)	0.12
Dominant model§										
PI4K2B or/and STIM2 up-regulated	88	62.9	1			70	64.2	1		
Both down-regulated	52	37.1	1.23	(0.68 – 2.22)	0.50	39	35.8	1.09	(0.52 – 2.28)	0.82

Abbreviations: HR, Hazard Ratio; CI, >Confidence Interval

† Regarding PI4K2B and STIM2, patients were divided in High or Low expression using the median value of the tumor/normal mRNA ratio as a cut-off

‡ Additive model summarizes the risk for the up-regulation of both genes in a given patient compared to the up-regulation of only one or none of the two genes

§ The dominant model summarizes the risk for the down-regulation of both genes in a given patient.

**P* values correspond to Cox proportional hazards regression models adjusted for tumor stage.

SUPPLEMENTARY INFORMATION

Figure 1S (A) Genetic map of 15.2-Mbp region of 4p14-16 flanked by D4S2633 and D4S3027 microsatellite markers. Thirty heterozygous microsatellite markers were selected from the human uniSTS database and ordered from the telomere (up) to the centromere (down). The genes defined for this region are shown in bold. **(B)** LOH analysis of some representative markers in all xenografted tumors. **(C)** Illustrative examples of LOH analysis. DNA from matched normal (N), primary tumor (T), and tumor or metastatic xenografts (X) were PCR amplified, and products were run in 6% polyacrylamide/8M urea denaturing sequencing gels at room temperature under 55 W for 2-3 h and silver stained. LOH was defined in xenografts by total loss of one allele, or by a markedly diminished staining intensity visible to the naked eye on inspection of any of the alleles. Allelic imbalances were observed in some microsatellite markers in two representative cases, CRC16 and HM15, whereas non-imbalances occurred in CRC2 and HM6. Human tumor cell enrichment in xenografts is shown by the lack of normal human stroma contamination. **(D)** Quantitative LOH analysis of microsatellite markers defining two inter-regions. Markers were amplified with fluorescent-labeled oligonucleotides running in ABI Prism 3770 equipment and analyzed with GeneMapper 3.0 software. Primers were labeled with FAM, VIC, NED and PET fluorochromes.

Figure S1

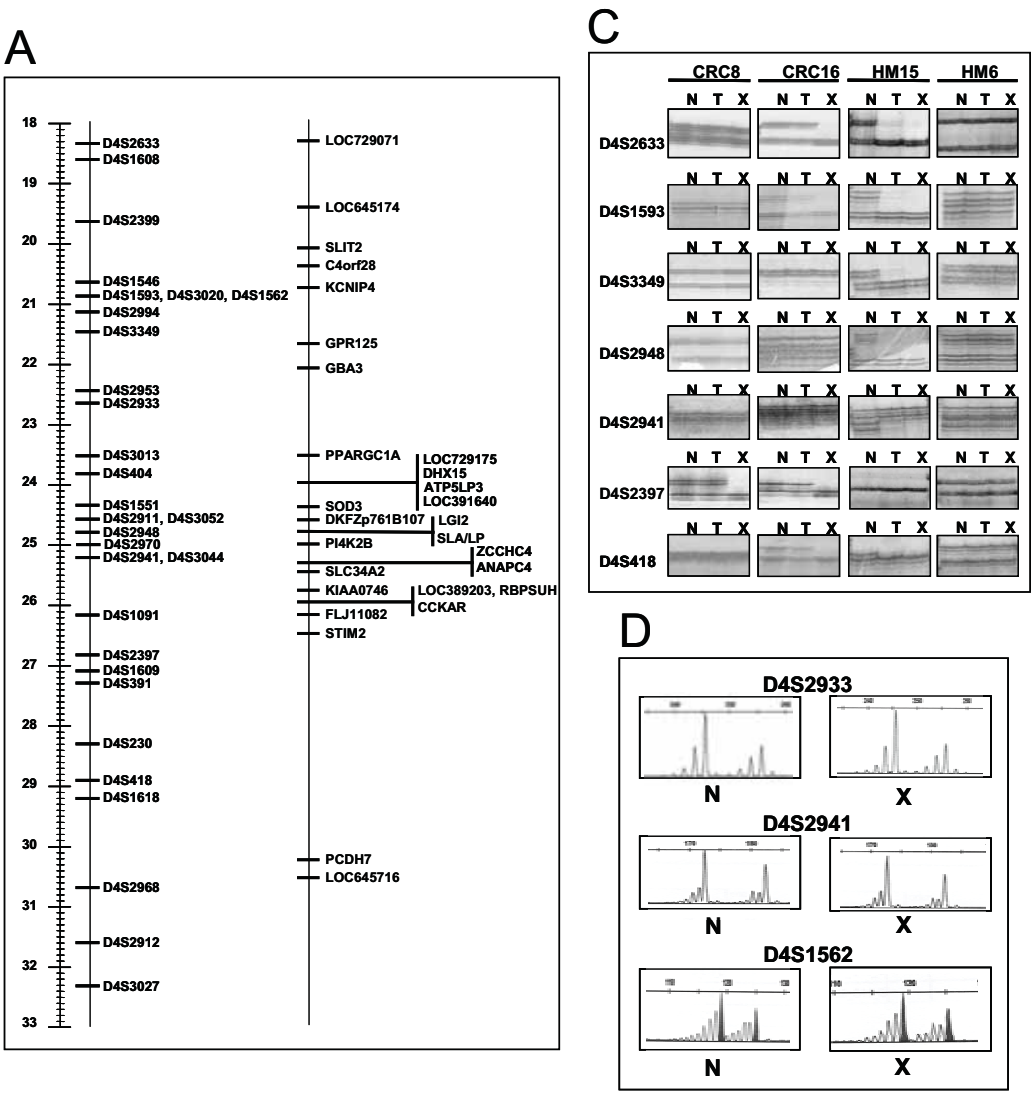
A
18
19
20
21
22
23
24
25
26
27
28
29
30
31
32
33
D4S2633
D4S1608
D4S2399
D4S1546
D4S1593, D4S3020, D4S1562
D4S2994
D4S3349
D4S2953
D4S2933
D4S3013
D4S404
D4S1551
D4S2911, D4S3052
D4S2948
D4S2970
D4S2941, D4S3044
D4S1091
D4S2397
D4S1609
D4S391
D4S230
D4S418
D4S1618
D4S2968
D4S2912
D4S3027
LOC729071
LOC645174
SLIT2
C4orf28
KCNIP4
GPR125
GBA3
PPARGC1A
LOC729175
DHX15
ATP5LP3
LOC391640
SOD3
DKFZp761B107
LGI2
PI4K2B
SLA/LP
ZCCHC4
ANAPC4
SLC34A2
KIAA0746
LOC389203, RBPSUH
FLJ11082
CCKAR
STIM2
PCDH7
LOC645716
C
CRC8
CRC16
HM15
HM6
N T X
D4S2633
D4S1593
D4S3349
D4S2948
D4S2941
D4S2397
D4S418
D
D4S2933
N
X
D4S2941
N
X
D4S1562
N
X

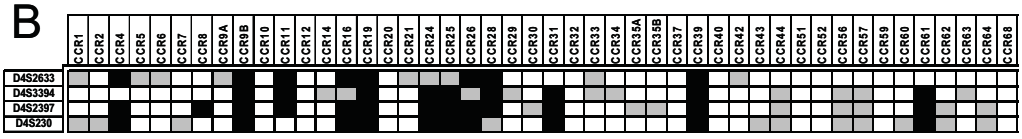
B
CCR1
CCR2
CCR4
CCR5
CCR6
CCR7
CCR8
CCR9A
CCR9B
CCR10
CCR11
CCR12
CCR14
CCR16
CCR19
CCR20
CCR21
CCR24
CCR25
CCR26
CCR28
CCR29
CCR30
CCR31
CCR32
CCR33
CCR34
CCR35A
CCR35B
CCR37
CCR39
CCR40
CCR42
CCR43
CCR44
CCR51
CCR52
CCR56
CCR57
CCR59
CCR60
CCR61
CCR62
CCR63
CCR64
CCR68
D4S2633
D4S3394
D4S2397
D4S230

Figure S2 Methylation status of 5' CpG promoter islands (CpGi). **(A)** The genomic region A includes 10 genes, from the most centromere-proximal, PI4K2B, to the most telomere-proximal, STIM2. CpG islands (CpGi) across this region are named according to the number of CpG residues that they contain. **(B)** Methylation data for four matched cases of normal colon mucosa (N) - primary colorectal tumor (CRC) - tumor xenografts (CRC-X) are summarized. Tumors CRC24 and -26 had high levels of PI4K2B and STIM2 expression as measured by qPCR, whereas CRC4 and -8 had lower levels. Each box represents a CpG island, which can be found unmethylated (white), partially methylated (grey), or heavily methylated (black). The image shows the results for twenty different CpG residues by island

Figure S2

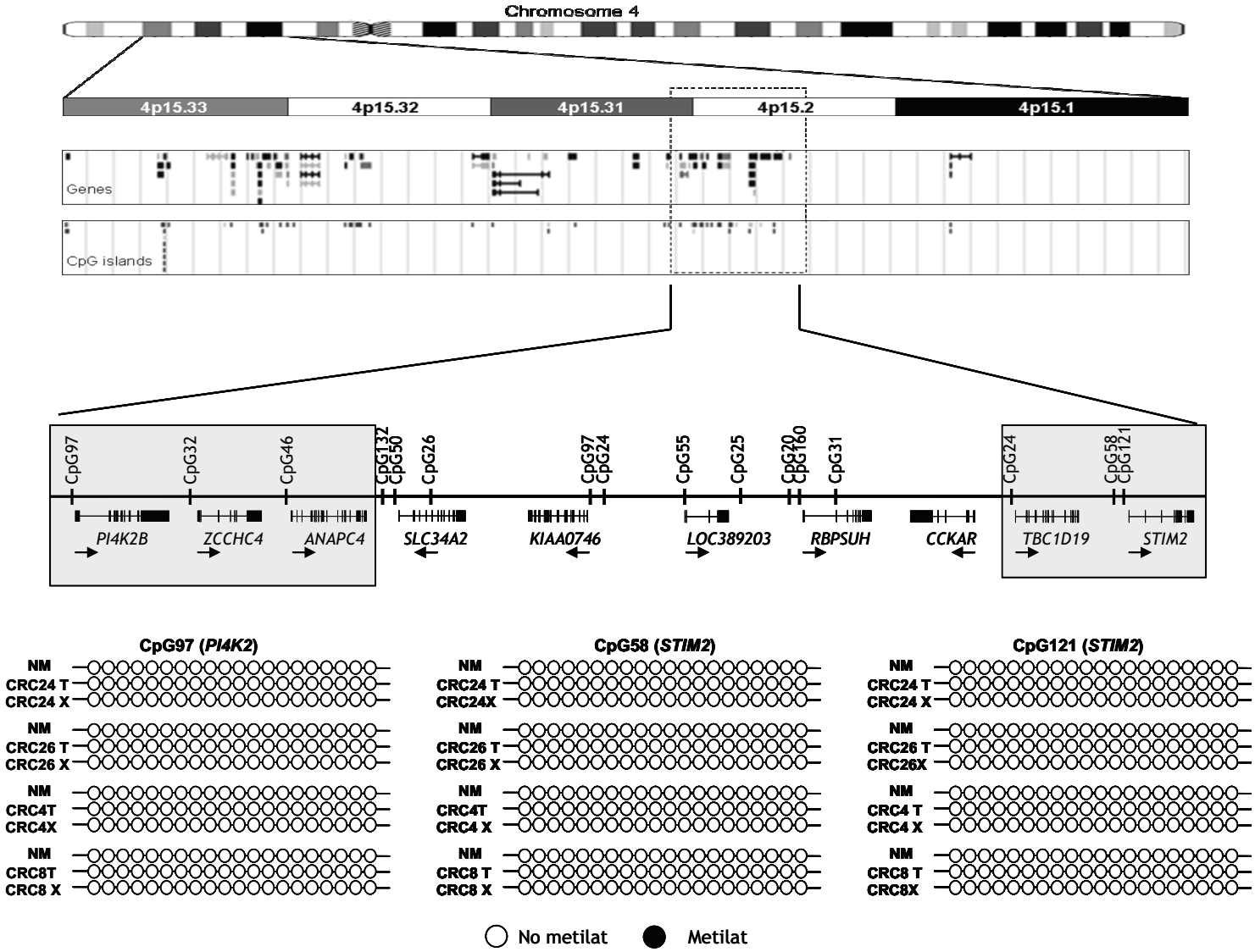
Chromosome 4
4p15.33
4p15.32
4p15.31
4p15.2
4p15.1
Genes
CpG islands
CpG97
CpG32
CpG46
CpG132
CpG50
CpG26
CpG97
CpG24
CpG55
CpG25
CpG20
CpG160
CpG31
CpG24
CpG58
CpG121
PI4K2B
ZCCHC4
ANAPC4
SLC34A2
KIAA0746
LOC389203
RBPSUH
CCKAR
TBC1D19
STIM2
CpG97 (PI4K2)
CpG58 (STIM2)
CpG121 (STIM2)
NM
CRC24 T
CRC24 X
CRC24X
CRC26 T
CRC26 X
CRC26X
CRC4T
CRC4X
CRC4 T
CRC4 X
CRC8T
CRC8 X
CRC8 T
CRC8X
No metilat
Metilat

Table S1 Individual clinicopathological characteristics of primary colorectal tumors.

Tumor	Age	Gender	Primary tumor histology	Location	Tumor T stage	Tumor Dukes' stage	Tumor xenograft [b]	Tumor dissemination in nude mice [c]
CRC1	66	F	Adenocarcinoma	Sigma	pT3c pN2	C2	+	No dissemination
CRC2	64	F	Adenocarcinoma	Sigma	pT3c pN2	C2	+	No dissemination
CRC3	54	F	Adenocarcinoma	Sigma	pT2 pN2	B1	-	-
CRC4	55	M	Adenocarcinoma	Sigma	pT3 pN0	B2	+	Lung metastasis
CRC5	56	F	Adenocarcinoma	Left	pT3 pN2	C2	+	Peritoneal implants
CRC6	55	F	Adenocarcinoma	Left	pT3 pN2	C2	+	No dissemination
CRC7	82	M	Adenocarcinoma	Sigma	pT3 pNx	B1	+	No dissemination
CRC8	74	F	Adenocarcinoma	Sigma	pT3 pN1	C2	+	Peritoneal implants
CRC9A [a]	82	F	Adenocarcinoma	Sigma	pT3 pN0	B2	+	No dissemination
CRC9B [a]	82	F	Adenocarcinoma	Sigma	pT2 pN0	B1	+	No dissemination
CRC10	72	F	Adenocarcinoma	Sigma	pT3 pN0	C1	+	-
CRC11	68	F	Adenocarcinoma	Sigma	pT4b pN2	C2	+	Lung metastasis
CRC12	46	M	Adenocarcinoma	Right	pT3 pN2	C2	+	Liver implants
CRC13	84	F	Adenocarcinoma	Rectum	pT3 pN0	C1	-	-
CRC14	73	F	Adenocarcinoma	-	pT4 pN1 M1	D	+	No dissemination
CRC15	82	M	Adenocarcinoma	Sigma	pT3 pN0	C1	-	-
CRC16	63	M	Adenocarcinoma	Right	pT3c pN1	C2	+	Liver implants
CRC17	56	M	Adenocarcinoma	Left	pT3 pN0	C1	-	-
CRC18	85	M	Adenocarcinoma	Rectum	pTis pN0	A	-	-
CRC19	78	F	Adenocarcinoma	Rectum	pT3 pN2	C2	+	Peritoneal implants
CRC20	74	M	Adenocarcinoma	Rectum	pT3 pN0 pM1	D	+	Liver implants
CRC21	77	M	Adenocarcinoma	Sigma	pT3 pN0	C1	+	nd
CRC22	42	M	Adenocarcinoma	Rectum	pT2 pN0	B1	-	nd
CRC23	74	M	Adenocarcinoma	Sigma	pT3 pN0	C1	-	nd
CRC24	72	M	Adenocarcinoma	Right	pT3 pN2	C2	+	nd
CRC25	66	M	Adenocarcinoma	Left	pT4 pN0	B2	+	nd
CRC26	82	F	Adenocarcinoma	Sigma	pT3 pN1	C2	+	nd
CRC27	73	M	Adenocarcinoma	Right	pT3 pN0	C1	-	nd
CRC28	63	F	Adenocarcinoma	Left	pT3 pN0	C1	+	nd
CRC29	79	M	Adenocarcinoma	Sigma	pT3 pN0	C1	+	nd
CRC30	74	M	Adenocarcinoma	Left	pT4 pN0	B2	+	nd
CRC31	71	M	Adenocarcinoma	Sigma	pT3 pN2	C2	+	nd
CRC32	76	M	Adenocarcinoma	Rectum	pT3 pN0	C1	+	Liver implants
CRC33	43	M	Adenocarcinoma	Right	pT3 pN1	C2	+	nd
CRC34	73	M	Adenocarcinoma	Right	pT3 pN0	C1	+	No dissemination
CRC35A [a]	72	M	Adenocarcinoma	Left	pT3 pN0	C1	+	nd
CRC35B [a]	72	M	Adenocarcinoma	Left	pT3 pN0	C1	+	nd
CRC36	67	M	Adenocarcinoma	Rectum	pT3 pN1	C2	-	nd
CRC37	78	M	Adenocarcinoma	Left	pT3 pN1	C2	+	nd
CRC38	72	F	Adenocarcinoma	Rectum	pT3 pN2	C2	-	nd
CRC39	80	M	Adenocarcinoma	Right	pT4 pN1	C2	+	nd
CRC40	76	F	Adenocarcinoma	Right	pT3 pN1	C2	+	nd
CRC41	72	M	Adenocarcinoma	Left	pT3 pN0	C1	-	nd
CRC42	69	M	Adenocarcinoma	Rectum	pT2 pN1	C1	+	nd
CRC43	82	F	Adenocarcinoma	Right	pT4 pN1	C1	+	nd
CRC44	70	F	Adenocarcinoma	Right	pT4 pN1	C1	+	nd
CRC45	65	F	Adenocarcinoma	Right	pT3 pN1	C1	-	nd
CRC46	82	M	Adenocarcinoma	Rectum	pT3 pN1	C1	-	nd
CRC47	72	F	Adenocarcinoma	Right	pT4 pN2	C2	-	nd
CRC48	63	M	Adenocarcinoma	Right	pT3 pN0	C1	-	nd
CRC49	60	M	Adenocarcinoma	Rectum	pT3 pN2	C2	-	nd
CRC50	57	F	Adenocarcinoma	Rectum	pT3 pN0	C1	-	nd
CRC51	42	M	Adenocarcinoma	Transverse	pT4 pN2	C2	+	nd
CRC52	83	M	Adenocarcinoma	Rectum	pT4 pN2	C2	+	nd
CRC53A [a]	69	M	Adenocarcinoma	Sigma	pT3 pN1	C1	-	nd
CRC53B [a]	69	M	Adenocarcinoma	Sigma	pT3 pN2	C1	-	nd
CRC54	84	M	Adenocarcinoma	Sigma	pT3 pN1	C1	-	nd
CRC55	64	M	Adenocarcinoma	Sigma	pT2 pN2	C1	-	nd
CRC56	68	M	Adenocarcinoma	Right	pT4 pN0	B2	+	nd
CRC57	25	F	Adenocarcinoma	Right	pT2 pN1	C1	+	nd
CRC58	63	F	Adenocarcinoma	Left	pT4 pN1	C1	-	nd
CRC59	66	F	Adenocarcinoma	Right	pT3 pN0	C1	+	nd
CRC60	72	F	Adenocarcinoma	Right	pT3 pN0	C1	+	nd
CRC61	78	M	Adenocarcinoma	Left	pT2 pN0	B1	+	nd
CRC62	74	F	Adenocarcinoma	Right	pT4 pN0	B2	+	nd
CRC63	71	F	Adenocarcinoma	Right	pT4 pN1	C1	+	nd
CRC64	37	F	Adenocarcinoma	Transverse	pT4 pN0	B2	+	nd
CRC65	86	M	Adenocarcinoma	Left	pT4 pN0	B2	-	nd
CRC66	78	M	Adenocarcinoma	Sigma	pT2 pN0	B1	-	nd
CRC67	80	M	Adenocarcinoma	Right	pT4 pN1	C1	-	nd
CRC68	63	M	Adenocarcinoma	Rectum	pT3 pN2	C2	+	nd
CRC69	71	F	Adenocarcinoma	Rectum	pT3 pN1	C1	-	nd
CRC70	56	M	Adenocarcinoma	Right	pT2 pN1	C1	-	nd

[a] Two independent primary colorectal tumors were obtained from the same patient.

[b] +, Primary colorectal tumor grew up as xenografted tumor in nude mice; -, tumor did not growth in mice.

[C] Distal dissemination in nude mice; -, tumor did not growth in mice; nd, non-determined.

Table S2 Individual clinicopathological characteristics of hepatic metastases.

Hepatic metastases	Gender	Age	Primary tumor location	Primary tumor T stage	Number of HMs	Type of metastases	Bilobar affection	Tumor xenograft [b]
MH1	F	68	Colon	IV	4	Synchronic	No	+
MH2	F	43	Colon	IV	4	Synchronic	No	+
MH3	M	63	Rectum	II	7	Metachronic	No	+
MH4	F	70	Rectum	IV	4	Synchronic	No	+
MH5A[a]	M	67	Rectum	III	3	Metachronic	No	+
MH5B[a]	M	67	Rectum	III	3	Metachronic	No	+
MH6	F	51	Rectum	IV	2	Synchronic	Yes	+
MH7	F	43	Colon	III	2	Metachronic	No	+
MH8	F	69	Colon	III	4	Metachronic	No	+
MH9	M	69	Rectum	IV	2	Synchronic	Yes	+
MH10	F	67	Rectum	IV	4	Synchronic	No	+
MH11	F	45	Rectum	IV	2	Synchronic	No	+
MH12	M	59	Colon	IV	3	Synchronic	No	+
MH13	M	76	Colon	II	1	Metachronic	Yes	-
MH14	M	75	Rectum	IV	1	Synchronic	Yes	+
MH15	F	57	Rectum	IV	>20	Synchronic	Yes	+
MH16	F	72	Colon	IV	2	Synchronic	No	+
MH17	M	69	Colon	IV	3	Synchronic	No	+
MH18	M	56	Colon	II	1	Metachronic	Yes	+
MH19	M	47	Colon	IV	1	Synchronic	Yes	+
MH20	F	42	Colon	IV	6	Synchronic	No	+
MH22	M	70	Rectum	II	1	Metachronic	Yes	-

[a] Two independent HMs were obtained from the same patient

[b] +, Hepatic metastasis grew up as xenografted tumor in nude mice; -, HMs did not growth in mice

Table S3 Clinicopathologic characteristics of patients with colorectal and hepatic metastases implanted in nude mice.

COLORECTAL TUMORS					HEPATIC METASTASES				
	Eligible patient's samples (N = 73)		Xenografted samples (N = 46)			Eligible patient's samples (N = 22)		Xenografted samples (N = 20)	
Characteristics	**No.**	**%**	**No.**	**%**	**Characteristics**	**No.**	**%**	**No.**	**%**
Age					**Age**				
? 69	31	42,4	18	39.1	?61	9	40,9	9	45
>69	42	57,6	28	60.9	>61	13	49,1	11	55
Gender					**Gender**				
Male	43	58,9	24	52.1	Male	11	50	9	45
Female	30	41,1	22	47.9	Female	11	50	11	55
Tumor location					**Primary location**				
Right Colon	21	28.7	15	32.6	Colon	11	50	10	50
Transverse Colon	2	2.7	2	4.3	Rectum	11	50	10	50
Left Colon	13	17.8	8	17.3	**Primary stage**				
Sigma	21	28.7	12	26	II	4	18,2	2	10
Rectum	15	20.5	6	13	III	4	18,2	4	20
Tumor differentiation					IV	14	63,6	14	70
Well	54	73,9	34	73..9	**Number of HMs**				
Poorly	16	21,9	11	23.9	<3	10	45,4	8	40
Missing	3	4.1	1	2.1	?3	12	54,6	12	60
Tumor stage					**Type of metastases**				
I or II	32	43,8	18	39.1	Synchronic	14	63,6	14	70
III	39	53.4	26	56.5	Metachronic	8	36,4	6	30
IV	2	2.7	2	4.3	**Bilobular affection**				
					Yes	8	36,4	6	30
					No	14	63,6	14	70

Table S4 FISH analysis of tumor touch imprints.

				Percentage (%) of nucleous			
		Sample	Probe	Wild-type	Deletion	Triploid	Tetraploid
Primary colorectal tumors	LOH at 4p-16	CRC4	23A21/ 372F2	nd	nd	nd	nd
			473F10/ 475J10	98	2	0	0
		CRC4-X	23A21/ 372F2	nd	nd	nd	nd
			473F10 /475J10	96	2	2	0
		CRC8	23A21/ 372F2	96	3	0	1
			473F10/ 475J10	93	4	1	2
		CRC8-X	23A21 /372F2	96	2	2	0
			473F10/ 475J10	98	2	0	0
		CRC11	23A21/ 372F2	97	3	0	0
			473F10/ 475J10	98	1	0	0
		CRC11-X	23A21 /372F2	98	1	1	0
			473F10/ 475J10	96	3	1	0
		CRC19	23A21/ 372F2	91	9	0	0
			473F10/ 475J10	96	3	0	1
		CRC19-X	23A21/ 372F2	98	2	0	0
			473F10/ 475J10	96	4	0	0
		CRC24	23A21/ 372F2	78	1	12	9
			473F10/ 475J10	68	0	25	9
		CRC24-X	23A21/ 372F2	nd	nd	nd	nd
			473F10 /475J10	nd	nd	nd	nd
		CRC25	23A21/ 372F2	97	0	3	0
			473F10/ 475J10	98	1	0	0
		CRC25-X	23A21/ 372F2	94	6	0	0
			473F10/ 475J10	98	2	0	0
		CRC26	23A21/ 372F2	98	1	0	1
			473F10/ 475J10	97	0	1	2
		CRC26-X	23A21/ 372F2	99	1	0	0
			473F10/ 475J10	97	2	1	0
		CRC28	23A21/ 372F2	20	80	0	0
			473F10/ 475J10	15	82	0	0
		CRC28-X	23A21/ 372F2	12	87	0	0
			473F10/ 475J10	15	85	0	0
	Without LOH at 4p14-16	CRC1	23A21/372F2	95	4	0	0
			473F10/475J10	96	3	0	1
		CRC5	23A21/372F2	95	3	0	2
			473F10/475J10	91	1	2	1
		CRC7	23A21/372F2	76	5	0	17
			473F10/475J10	70	3	0	27
		CRC9A	23A21/372F2	93	2	5	0
			473F10/475J10	92	3	0	5
		CRC10	23A21/372F2	93	3	0	4
			473F10/475J10	50	1	47	2
		CRC12	23A21/372F2	95	4	0	1
			473F10/475J10	96	4	0	0
		CRC14	23A21/372F2	99	1	0	0
			473F10/475J10	98	2	0	0
		CRC20	23A21/372F2	95	3	1	1
			473F10/475J10	97	2	1	0
		CRC21	23A21/372F2	94	5	0	1
			473F10/475J10	95	3	1	2
Hepatic metastases	LOH at 4p14-16	HM3	23A21/372F2	92	4	4	0
			473F10/475J10	94	2	4	0
		HM10	23A21/372F2	98	0	0	2
			473F10/475J10	nd	nd	nd	nd
		HM10-X	23A21/372F2	88	4	8	0
			473F10/475J10	12	85	0	0
		HM12	23A21/372F2	58	2	48	2
			473F10/475J10	76	0	28	0
		HM12-X	23A21/372F2	63	2	30	5
			473F10/475J10	67	0	30	3
		HM15	23A21/372F2	12	0	78	0
			473F10/475J10	8	1	82	0
		HM15-X	23A21/372F2	19	1	80	0
			473F10/475J10	7	0	91	0
		HM20	23A21/372F2	nd	nd	nd	nd
			473F10/475J10	nd	nd	nd	nd
		HM20-X	23A21/372F2	97	1	1	1
			473F10/475J10	96	2	1	1

CRC, Primary colorectal tumor; CRC-X, Xenografted colorectal tumor; HM, Hepatic metastasis; HM-X, Xenografted hepatic metastasis.
nd, not determined .

Table S5 Microsatellite markers at 4p14-16 analyzed in colorectal tumors.

Markers	Primers	Amplicon size (bp)	Tm (ºC)	Chromosome 4 map position
D4S3360	Forward CTAGCTTTGATTCTATTGACC Reverse GGTCTAAATCAATGACCTAAGC	175 - 199	55	105905 - 106080
D4S133	Forward GTGAGCAGAGCAAAGTCTCAGG Reverse AGTGACAGAGTGAGGCTCTCGT	239 - 259	56	678759 - 679013
D4S1614	Forward CATCTAGGAGAATCAGTACTTGG Reverse TTACCATGAGCATATTTCCA	143 - 149	58	2616508 - 2616654
D4S3034	Forward CTGCCAATAAACTGGGT Reverse TTGCTCACCAAAGAGGTT	182 - 188	57	3295334 - 3295520
D4S3023	Forward ACCTCACTGGAAACTAAATGG Reverse TGAACAGCAGCGGTCT	125 - 155	54	4352370 - 4352514
D4S431	Forward CAAAACTTATGTTACTGTCCCATGC Reverse CCATCAGCGTCTTCGTTATACTC	151	53	6466546 - 6466696
D4S2366	Forward TCCTGACATTCCTAGGGTGA Reverse AAAACAAATATGGCTCTATCTATCG	120 - 140	55	6535686 - 6535816
D4S2935	Forward GCTCACAGAAGTGCCCAATA Reverse CCCTGGGTGAAGTTTAATCTC	104 - 120	57	6611978 - 6612093
D4S394	Forward CCCTTGAGCATCCTGACTTC Reverse GAGTGAGCCCCTGTACTCCA	189 - 223	57	7010929 - 7011125
D4S2983	Forward TGTCCAGTTGGCAGGG Reverse GGTCGCATTCATTCGC	212 - 254	52	7796366 - 7796619
D4S2928	Forward ATAGACGTGTTCCTGGTGG Reverse CTCAGGCTATTTATGGGGTG	161 - 201	57	10221409 - 10221607
D4S1582	Forward ATCAGGGTTCTCCACACAAA Reverse TTGGTTGAAACTTGTGGATATAAA	112 - 126	56	10310683 - 10310794
D4S1605	Forward CATTCTAGTAGTTATTGGCTTATCC Reverse CAGTTGCTTGATACCTATATTTTTC	127 - 133	57	10661280 - 10661407
D4S3009	Forward ATGGCCTGTGAATCAACCC Reverse AATCCTTTGAAGACGGCCC	261 - 279	57	10745945 - 10746217
D4S3036	Forward AGCTTCTTGCTGTGTCC Reverse AAGGGTGGGGCTCTAT	162 - 178	52	-
D4S2906	Forward CAGTCTAGATTCAAAGGAATTAGAC Reverse AATTAGAGATGCCCGTGAAA	164 - 176	55	12321269 - 12321440
D4S2944	Forward AGATTCTGGCCTCCTTGC Reverse CCTGGTGAAGTGGTGGG	124 - 150	57	13140729 - 13140874
D4S403	Forward AGGTGGCCCTGAGTAGGAGT Reverse TTTGAGGGAATGATTTGGGT	217 - 231	56	13360044 - 13360264
D4S2942	Forward CAAATGCCCATCAATCAAC Reverse GGGTCCAGTCTCATCCAC	151 - 163	56	13380180 - 13380330
D4S1602	Forward CCAGATGGGTTCCAAATGA Reverse TGTGGACTGAGTAGAGAGTGCC	222 - 233	56	14058331 - 14058553
D4S2362	Forward TAAATATTGGTAGGATGAATGAATG Reverse CCCATCCCGTTACCTCTTTA	146 - 154	56	15067035 - 15067178
D4S2960	Forward AAGGCTTTATCATTAAGAATCCTA Reverse TGAGGGTATAGTTACCATCTTTT	233 - 249	54	15437088 - 15437326
D4S1601	Forward AACTGGCTTCCCCACC Reverse TCGGGCTACTTTTGGCTA	124 - 146	54	15630532 - 15630663
D4S1567	Forward GCTCCTTGCCACTTAATGTA Reverse CTAGGTCTGCCTGATTCTAAAGT	100 - 114	57	16064527 - 16064640
D4S2642	Forward TGAGCTTGCTCTCCTATGCT Reverse TCACTTCAGAGCACACAGGA	228 - 244	57	16128493 - 16128734
D4S2926	Forward TTAACCAGTGGAGGCCAGT Reverse CTCTTAAAGAACAGGGTGTCTGATA	181 - 199	56	17076708 - 17076888
D4S2946	Forward GTCAAGAGGGCTGATTCTG Reverse ACCTGTCTGAACTTGCGTG	104 - 126	56	17362511 - 17362618
D4S2633	Forward AAGGTTCCAGGACACATTCA Reverse CCTGGATCTCCAGCTTACAA	200 – 233	58	18454310 - 18454532
D4S1608 *	Forward GAAAATGCTGCCTGGGA Reverse AAGGAATTACTAGCCCATAAAGGT	231 – 247	60	18696600 - 18696764
D4S2399 #	Forward CAAAGGCAGCCTTTATTTCA Reverse CACAGGGACACAGGGAGG	305 – 313	58	19673341 - 19673646
D4S1546 †	Forward CTACCGACTAGAATCACATGGG Reverse GACCTGTCCAAACGCCT	146 – 160	58	20375375 - 20375522

D4S3020 #	Forward Reverse	TCCTGTTTGAGTGTTTAGACATTGC TATCCTGCTGATTGAAAGTTTGGC	113 – 135	58	20870569 - 20870689
D4S1562	Forward Reverse	GATCACAGTCCTGAACTCAGAAC TACCTGTAATTGCACTAGCAAATCC	220	50	20892896 - 20893113
D4S2994 †	Forward Reverse	TTAACCTTGGTGATGTTCATAGAC GCAGCAATTATGGGCTGT	127 – 179	58	21112356 - 21112504
D4S3349	Forward Reverse	GTGTGTTGTATGTGTGTATGCG CACCGCCACATAGAGAGATA	134 – 154	58	21480426 - 21480572
D4S2953	Forward Reverse	TCCAAAAAAACAAGGTCAGA CTCATTGATGGGCTACTCATTA	142 – 150	54	22506270 - 22506415
D4S2933 ‡	Forward Reverse	AGTCTGCTTGAGAGGGTCTATCTT TAACGAAACTGGACTGACGA	213 – 223	58	22671247 - 22671465
D4S3013	Forward Reverse	GAACACTCTCCCATTATGCT TTAAGTGACCTGGGTCAATAA	144 – 164	58	23506627 - 23506790
D4S404	Forward Reverse	CTCATTTACCTGCACTAAGAGGAC CTAGAGAAGGAAGAGAAATGTTTGG	88 – 101	58	23844269 - 23844412
D4S1551	Forward Reverse	GACCTTGTGAGCGTGTGAGT AGTCAGGGTTCTCCAGAGAAAT	172 – 186	64	24360159 - 24360332
D4S2911 *	Forward Reverse	TGCCATGTTAAGTGGGG ATTTGGGTGCATTTGGTC	181 – 189	58	24449652 - 24449840
D4S3052 #	Forward Reverse	TCACAGATGCCAGAGCAAG CCCAGTCCCACTCACAAG	104 – 130	57	24486974 - 24487099
D4S2948 †	Forward Reverse	TGCAGGCTAAGTATGTTCCA TTCCCGGCTCTGTAACAC	134 – 154	58	24618236 - 24618385
D4S2970 ‡	Forward Reverse	GTACCAGCCAGATGTATTTATCTTG TTCCTGCCTGAATATGATGC	152 – 178	58	24918149 - 24918322
D4S2941 *	Forward Reverse	TGTGTATACCTAAGAAATGCAAAT GTACCTGGCGTAGAACAAGT	145 – 183	58	25166501 - 25166679
D4S3044	Forward Reverse	AGCTCATGATTATGTAAACCATG TCTTGCTCCATCCACC	143 – 175	58	25189107 - 25189273
D4S1091	Forward Reverse	CCCAAAACTGGTTCATTGAT TTACCATTTCTGATAATGGTAAC	127 – 137	53	26207151 - 26207282
D4S2397 *	Forward Reverse	CATGCACACCAAAACAAGAA GCAACAAACCTGCACATTCT	126 – 144	58	26866965 - 26867101
D4S1609	Forward Reverse	TCTGAAAATGCCCTTGACC CATCATTACTGCTGGGATGC	163 – 177	56	27082728 - 27082900
D4S391 ‡	Forward Reverse	CACATAACTTCCCTTGCTGG ACTGTTGTCAAATCAGGCTC	164 - 185	53	27221546 - 27221759
D4S230	Forward Reverse	TAGGAATAGGAAACAAATGCA TTAGGATGCTGACTTCACCA	191 – 217	54	28248567 - 28248762
D4S418	Forward Reverse	CTATGATTTGTATGTTTGTTTCACCC TCAGGCTTTTTTTAACAACCAACTC	210 – 226	58	28974395 - 28974586
D4S1618 #	Forward Reverse	GCTTTGTCCCTACTTTCCTGTTG ATGTGAGTATAATGGATGGTGTATG	160	55	29118970 - 29119129
D4S2968 †	Forward Reverse	GATCTACAAGTAATTCACTGTAGCA CATTTTGTGATTTGATGTTAGTCAG	170 – 186	56	30781930 - 30782103
D4S2912 ‡	Forward Reverse	AGCTAAACCATTATGGCAT TCTAGTTAATTCTCCGTTTCAT	192 – 238	51	31644444 - 31644665
D4S3027	Forward Reverse	CCTTGCATCATCAATGTTT TGAATGGGTCTATCTGGTG	132 – 156	58	32339840 - 32339991

Primers were labeled with * FAM; # VIC; † NED; and ‡ PET fluorochromes and PCR products were resolved with an automatic sequencer and results analyzed with GeneMapper software.

Table S6 Primers for analysis of 5'CpG promoter islands.

CpG Island [#]			Primers	Amplicon size (bp)	Annealing temperature (ºC)
CpG97.1	External	Forward	TTTTTGGTTGTAGGAGGG	312	54/56
		Reverse	GAAACCAAATCAAAACAACCA		
	Internal	Forward	GGGAGTAAAGTGAGTTGT		54
		Reverse	ATACCAAAAACTAAACTCT		
CpG97.2	External	Forward	TGTAGAGTTTAGTTTTTGG	276	54/56
		Reverse	CAAAACCGAATCACACCTAA		
	Internal	Forward	TGGTTGTTTTGATTTGGTTTCA		54
		Reverse	AACTCCGAAAAACCCCCA		
CpG32	External	Forward	TATTTTTAAGAAAGGAGGGTG	387	54/56
		Reverse	TTCCAAACCAACTCACACC		
	Internal	Forward	GTGTTGAGTTTATGGTATAGG		54
		Reverse	CTAAACCCAAACTCTAACC		
CpG46.1	External	Forward	GTTTTTTGTTTTGTTTATGGG	329	54/56
		Reverse	CAAACCAAAAAAATAATCTCCT		
	Internal	Forward	GGTTTTTAGTTTTAAGA		52
		Reverse	TACTTCTCTCCCACCACC		
CpG46.2	External	Forward	GGTGGTGGGAGAGAAGTAG	247	54/56
		Reverse	TAACACAAACATCACCTTTC		
	Internal	Forward	AGGAGATTATTTTTTTGGTTTGG		54
		Reverse	CTTAAAATTTACTACCATCCT		
CpG24	External	Forward	TGTGGTTTTGAAAGAATGAG	299	54/56
		Reverse	CCCTTAAACTTTTAAACTATCT		
	Internal	Forward	TAATTATAGATAAGGTAGGAA		54
		Reverse	TCCTCCTACAACATTTCCC		
CpG58.1	External	Forward	GTTTTATTGATTGAATGGAG	384	54/56
		Reverse	AATTCTCAAACTACTAAATTC		
	Internal	Forward	GTTTATATTATTTTAGAGGTGT		54
		Reverse	ACTCCCACTCTATAAA		
CpG58,2	External	Forward	AAGGAGAAGATTAGTGGGA	382	54/56
		Reverse	CAAAAACAAACCTACCCT		
	Internal	Forward	GAATTTAGTAGTTTGAGAATT		54
		Reverse	CCTATCTCCCTCTTCTCC		
CpG121.1	External	Forward	TAAATAGTTAGTTATTTGTAAG	349	54/56
		Reverse	AAACGCCTCCCTCCCCT		
	Internal	Forward	TTGAAATTATGGGGATGTTG		58
		Reverse	CCTCCCTCAAACTCTCCA		
CpG121.2	External	Forward	GGGCGGGGTTGGGATGT	339	54/56
		Reverse	CCCCGCCGCCTCAAACA		
	Internal	Forward	TGGAGAGTTTGAGGGAGG		58
		Reverse	CCAACCTAATCCCAT		
CpG121.3	External	Forward	GGATTAGAGTTTCGGAGGT	383	54/56
		Reverse	AAAATACTAACCTCTACA		
	Internal	Forward	GTGTCGATGGGATTAGGTTGG		56
		Reverse	CCCCTCACCTATCATAAA		
CpG121.4	External	Forward	GGTTGTTGGTAGTCGGAG	288	54/56
		Reverse	CAAACCCTACTAACACTTC		
	Internal	Forward	TTTATGATAGGTGAGGGG		56
		Reverse	AAAAACCACCACATTACTCAAC		

[#]CpG Islands with longer size than 300-350 bp were analyzed by overlap PCR reactions.